OPTIMIZER SELECTION BASED ON FUNCTION-PROXY PROXIMITY

Anonymous authors
Paper under double-blind review

ABSTRACT

Many machine learning problems involve the challenging task of training a model to fit the training data; this task is especially challenging for nonconvex problems. Many model training algorithms have been proposed, but it is often difficult to determine which algorithm is best suited to a given machine learning problem. To contend with this challenge, we study the effect of loss function curvature shift on optimizers' proxies of the loss function, and obtain a bound on the rate at which a very large family of optimizers (including all of the most prevalent ones) descend towards the loss function's minimum, while only making relatively weak assumptions on the loss function. Uniquely, our bound is tight even in parameter subspaces in which the loss function is concave, which have been shown to bear potential for fast descent while being neglected by existing convergence rate bounds. We demonstrate the applicability of our bound by developing a meta-algorithm for optimizer selection based on it, and validate our meta-algorithm experimentally.

1 INTRODUCTION

Machine learning problems involve training a model to fit a target distribution (such as protein structures, image labels, text, etc.), usually given as a set of samples from said distribution. However, no single existing training algorithm (a.k.a. "optimization algorithm", or "optimizer") is best suited to all machine learning problems - each has its unique strengths and weaknesses (see Vaswani et al. (2020); Sivan et al. (2024); Ruder (2016); Mustapha et al. (2021); Bera & Shrivastava (2020); Zeiler (2012); Duchi et al. (2011b); Xu et al. (2017); Wadia et al. (2021); Mittal et al. (2019); Zhou et al. (2020); Schmidt et al. (2021)), such as generalization capability, convergence rate, saddle-point and flat region evasion capability, robustness to hyperparameter choice, computational complexity per-iteration, memory complexity, etc., and different areas in which it empirically seems to work best. This diversity of optimizers raises the question of how to select an optimizer for a given problem; ideally, we would like to have a meta-algorithm for optimizer selection. Moreover, since the best optimizer may vary throughout the training process and among different model parameters, our ideal algorithm should combine optimizers by continually selecting the best optimizer for each individual parameter online, all throughout the training process.

One way to compare the computational overheads of different methods is experimentally; the literature is rich with such experiments on a variety of applications (Xu et al., 2017; Schmidt et al., 2021). On the theoretical side - convergence rate bounds have been proven for various optimizers. However, due to the wide variety of assumptions, convergence rate metrics, bound parameters (which may be expensive - if not impossible - to compute ahead of time), and tightness of the bounds in all of these works, comparing amongst them and applying these bounds for optimizer selection remains a challenging task. Existing bounds are also rarely applicable to novel optimizers, and are insufficiently tight, as may be seen by their failure to demonstrate the empirically-verified faster convergence of the more sophisticated methods that make use of second-order curvature information instead of exclusively gradients. Lastly, most broadly applicable bounds for non-convex functions fail to sufficiently address the rate of curvature change across the loss function surface. One particular area that suffers from neglect is linear subspaces of the parameter space in which the loss function is concave (meaning that a restriction $f|_{\mathbb{S}} : \mathbb{S} \to \mathbb{R}$ of the loss function f to a linear subspace $\mathbb{S}$ is locally concave). We believe that more attention should be given to these subspaces in the context of neural network optimization; Alain et al. (2018) and Ghorbani et al. (2019) experimentally demonstrate that

there is much to be gained by taking optimal steps in these subspaces, with gains that are often orders of magnitude greater than the potential gains in convex subspaces.

Our contributions

1. We design a new and refined cubic approximation which gives rise to an easy to compute algorithmic baseline named ELMO (Alg. 1), and prove its minmax-optimality[1] up to the third order. We also show the equivalence between our approach and a special preconditioning matrix which results in a natural refinement of Newton's method.
2. Based on this algorithmic baseline, we design a novel meta-algorithm named AMOS (Alg. 2) that enables us to adaptively select between first and second order training methods in order to boost performance.
3. We present an experimental study on NanoGPT that demonstrates AMOS's applicability in practice.
4. We present an experimental study of the Hessian's rate of change throughout training.

Our paper is organized as follows: In section 2, we review previous work and describe the notation we will use throughout the paper. In section 3, we develop the ELMO algorithm and use it as a baseline for an analysis of arbitrary quasi-Newton optimizer regret. In section 4, we use the bounds we developed to construct a meta-optimizer that selects the appropriate optimizer on-the-fly. Its performance is demonstrated experimentally. Finally, in section 5 we show the value of our novel Lipschitz parameter separation scheme by showing that the Hessian-Lipschitz parameters of certain eigenspaces are much smaller than others, giving optimizers a more accurate loss-function proxy.

2 BACKGROUND

Assumption 1. *For a given optimization problem with loss function $f : \mathbb{R}^n \to \mathbb{R}$, we assume f is twice differentiable.*

We note that this assumption is satisfied for all prevalent deep learning optimization problems for all but a zero-measure set of parameters.

2.1 NOTATIONS AND DEFINITIONS

Notation 1. Let $\theta_{t+1}, \theta_t \in \mathbb{R}^n$ the parameter vectors of a pair of consecutive iterations of a given optimization algorithm.

- For brevity of notation, we mark $\Delta\theta_t \triangleq \theta_{t+1} - \theta_t$.
- We mark $\nabla f(\theta_t)$ the gradient of f and $\mathcal{H}(\theta_t)$ the Hessian of f at θ_t.

Notation 2. Let $\theta_t \in \mathbb{R}^n$. We mark $(v_i(\theta_t), \lambda_i(\theta_t))_{j=0}^n$ an orthogonal eigendecomposition of $\mathcal{H}(\theta_t)$ (which exists due to the Hessian symmetry property). For brevity of notation, we will sometimes drop the (θ_t) and just write v_i, λ_i when the meaning is clear.

Since v_i and $-v_i$ are both equally viable eigenvectors, we eliminate ambiguity by assuming

$$\forall_{i\in[n]} : \nabla f(\theta_t)^\top v_i \leq 0 \tag{1}$$

with $\top$ indicating transposition.

Definition 1. We say an algorithm is a *k-order algorithm* if it requires oracle access to the first k derivatives of f.

[1] Given an optimization algorithm, there exists an "adversarial" loss function that minimizes the descent obtained by this optimizer, while matching all of the information gathered about the loss-function at a given iteration. We define "regret" as the difference between the actual descent obtained by a given algorithm in this adversarial setting, and the descent obtainable by the most adversary-robust algorithm (meaning that it maximizes loss function descent despite the adversary). An algorithm that computes the minimizer of this regret at each iteration is called "minmax-optimal".

Notation 3. For $\tau \in \mathbb{N}$ we mark $[\tau] = \{t \in \mathbb{N} : t \leq \tau\}$.

Definition 2. Let $U, D \in \mathbb{R}^{n \times n}$ s.t. $D = \textit{diag}\left(d_1, d_2, \ldots, d_n\right)$ is diagonal and U orthogonal, and let $\xi : \mathbb{R} \to \mathbb{R}$. We mark $\xi\left(U \cdot D \cdot U^\top\right) = U \cdot \textit{diag}\left(\xi\left(d_1\right), \xi\left(d_2\right), \ldots, \xi\left(d_n\right)\right) \cdot U^\top$.

Notation 4. Let $A, B \in \mathbb{R}^{n \times n}$. We write $A \succeq 0$ iff A is positive semi-definite, $A \succ 0$ if A is positive definite, $A \succeq B$ if $A - B \succeq 0$ (and likewise for $A \succ B$).

Definition 3. We say that an optimization algorithm is a *quasi-Newton optimization algorithm* if its characteristic update rule may be expressed as:

$$\theta_{t+1} = \theta_t - \alpha_t \Phi_t \nabla f\left(\theta_t\right)$$

for $\Phi_t \in \mathbb{R}^{n \times n}, \Phi_t \succeq 0, \Phi_t^\top = \Phi_t, \alpha_t \in \mathbb{R}^+$. We call Φ_t in such algorithms the "preconditioner matrix".

This approach is inspired by Newton's method in convex optimization (see Nocedal & Wright (2006, Chapter 3)) where $\Phi_t = \left(\mathcal{H}\left(\theta_t\right)\right)^{-1}$; see appendix A for a discussion of the challenges and proposed solutions involved in these algorithms. The overwhelming majority of gradient-based optimizers may be expressed as quasi-Newton optimizers (see Martens (2020) for examples), so this paper will concern itself exclusively with this family of optimizers.

Notation 5. Throughout this paper, we will mark the point a convergent quasi-Newton algorithm converges to by θ^*.

2.2 Related work

The value of the loss function after t iterations is of particular importance to practitioners, due to its implications on the quality of model. One measure of optimizer quality relating to this value is the objective function sub-optimality gap (OFSOG), defined as $f\left(\theta_T\right) - f\left(\theta^*\right)$. The ARC algorithm is a second-order algorithm that uses a low-rank SVD approximation of the Hessian and estimates a single Hessian-Lipschitz parameter adaptively; Cartis et al. (2012b) prove that OFSOG-optimality (bounding the OFSOG to below ϵ) is achieved by a variant of the ARC algorithm after $\mathcal{O}\left(\epsilon^{-1}\right)$ iterations in the convex regime, or $\mathcal{O}\left(\log\left(\epsilon^{-1}\right)\right)$ iterations in the strongly convex regime. Garmanjani (2020) show similar bounds for the Nonlinear Stepsize Control algorithm family, and Toint (2013) demonstrate that this is a generalization of ARC and trust-region methods. Liu et al. (2024) prove OFSOG-optimality for the Sophia optimizer (a second-order algorithm that approximates the Hessian as a diagonal matrix, which is estimated with Hutchinson's estimator (Hutchinson, 1989)) after $\mathcal{O}\left(\epsilon^{-1}\right)$ iterations in the convex regime.

Bottou (2004) partition the optimization process into the initial "search phase", in which the optimizer searches for an approximately convex region in which a local minimum resides, and the later "final phase", in which the optimizer converges to this local minimum.

In the machine learning literature, many common loss functions are "empirical risk functions" - that is, loss functions which can be written as a sum of terms, each of which is a function of only a single sample from the data distribution. When this sum ranges over a very large number of samples, a common approach to estimating it is to perform a Monte Carlo approximation, summing over only a small subset of the terms; this approach is known as the "minibatch approach". Amari (1998) then note that when using this approach, θ_t may be seen as a statistical estimator for θ^*. Working in the "final phase" (and thus assuming convexity), and adopting the estimator approach to θ_t taken by Amari (1998); Bottou & Lecun (2004) give a convergence rate bound for this estimator's variance parameterized by the first- and second-order derivatives at θ^*, assuming only that $\lim_{t \to \infty} \Phi_t = \mathcal{H}^{-1}\left(\theta^*\right)$. Martens (2020) takes these convergence rates and plugs them into a Taylor approximation of $f\left(\theta_t\right)$ to obtain the asymptotic OFSOG, given by $f\left(\theta_T\right) - f\left(\theta^*\right) = \frac{n}{2T} + o\left(\frac{1}{T}\right)$.

Since the goal of optimization is to minimize a loss function, arguably the best metric for measuring an optimization algorithm's quality are the gains it makes as measured by the loss function values, i.e. its rate of loss function descent. Nevertheless, most algorithms' convergence rate bounds relate to their gradient norms; we note, however, that a bound on an algorithm's gradient norm may be a poor proxy for its descent rate in the early, nonconvex "search" phase, since convergence rate bounds may only imply proximity to a critical point of the gradient, which is neither guaranteed to be the point the algorithm will ultimately converge to nor even to have a small loss function value by any measure.

To the best of our knowledge, our bound is the first to directly address the problem of bounding the loss function value in the "search" phase without assuming convexity (despite neural network loss functions rarely being convex in practice).

We refer the reader to appendix B for discussion on previous attempts at universal convergence rate bounds, other convergence rate measures, and the effect of the preconditioner (and correspondingly, the effect of optimizer choice) on convergence rate.

3 A MINMAX HESSIAN LIPSCHITZ-AWARE OPTIMIZATION ALGORITHM

Optimization algorithm iterations are comprised of two parts: first, we gather information about the loss function and construct a local model of the loss function, and second - we step to the minimum of this proxy. Accordingly, gradient descent and Newton's method use first- and second-order Taylor approximations of f respectively, and while these proxies do give a direction of descent in every subspace of the domain space, they do not indicate optimal step sizes in concave subspaces of the domain space (that is, subspaces in which the loss function is locally concave), since concave first- and second-order polynomials have no minima. To obtain a unique step in all settings (so that our optimizer will be sufficiently general to apply to nonconvex and nonquadratic regions of neural network loss functions), we must therefore model f with a third-order Taylor polynomial.

3.1 GENERAL BOUNDS ON PER-ITERATION DESCENT

A recurring theme in the neural network optimization literature is that the greatest-magnitude eigenvalues of the Hessian are slow to change, as well as their eigenvectors; see, for instance, Sivan et al. (2024); Alain et al. (2018); Sagun et al. (2016); Ghorbani et al. (2019); Gur-Ari et al. (2018); Liu et al. (2024). It is common to formalize this as an assumption (see, e.g., O'Leary-Roseberry et al. (2019); Nesterov & Polyak (2006)) of Hessian-Lipschitz continuity with the matrix spectral norm:

$$\exists_{L_H \in \mathbb{R}} \forall_{\theta,\varphi \in \mathbb{R}^n} : \|\mathcal{H}(\theta) - \mathcal{H}(\varphi)\|_2 \leq L_H \cdot \|\theta - \varphi\|_2 \tag{2}$$

This assumption relies on a single scalar $L_H \in \mathbb{R}$ to describe the the entire Hessian's rate of change. With $\frac{n^2}{2}$ independent entries, however, the Hessian can shift in a far more subtle manner, leading this assumption to be overly conservative, requiring a very large L_H for the assumption to be satisfied, which leads to looseness in convergence rate bounds and suboptimal performance of algorithms that rely on this scalar. We instead make the following finer-grained assumption on the rate of change of the Hessian's eigendecomposition:

Assumption 2. *Hessian Lipschitz-Continuity in each Eigenspace*

For any $\theta, \varphi \in \mathbb{R}^n$, let (eigendecompositions) $\mathcal{H}(\theta) = V \cdot \Lambda \cdot V^\top, \mathcal{H}(\varphi) = \tilde{V} \cdot \tilde{\Lambda} \cdot \tilde{V}^\top$ with $V, \tilde{V} \in \mathbb{R}^{n \times n}$ orthogonal matrices and $\Lambda = diag\left(\lambda_i\right)_{i=1}^n, \tilde{\Lambda} = diag\left(\tilde{\lambda}_i\right)_{i=1}^n \in \mathbb{R}^{n \times n}$ diagonal matrices, sorted s.t. $\forall_{i \in [n-1]} : \lambda_i \leq \lambda_{i+1}, \tilde{\lambda}_i \leq \tilde{\lambda}_{i+1}$. Then the following are satisfied:

$$\forall_{\theta \in \mathbb{R}^n} \exists_{\left(\bar{L}^i\right)_{i=1}^n \in (\mathbb{R}^+)^n} \forall_{\varphi \in \mathbb{R}^n} : \left|\lambda_i - \tilde{\lambda}_i\right| \leq \bar{L}^i \cdot \left|(\theta - \varphi)^\top v_i\right|$$

$$\forall_{\theta \in \mathbb{R}^n} \exists_{L_R \in \mathbb{R}^+} \forall_{\varphi \in \mathbb{R}^n} : \left\|V - \tilde{V}\right\|_2 \leq L_R \cdot \|\theta - \varphi\|_2$$

$$\exists_{L_H \in \mathbb{R}} \forall_{\theta \in \mathbb{R}^n} \forall_{i \in [n]} : \max\left\{L_R, \bar{L}^i\right\} \leq L_H \wedge \bar{L}^i \geq L_H^{-1}$$

When θ is the t-th iterate θ_t of an optimization algorithm, we'll mark the corresponding Lipschitz parameters as L_t^i. We will experimentally demonstrate the significance of this refinement later, by demonstrating that these parameters vary by orders of magnitude.

The above assumption allows us to bound the loss function in each eigenspace of the Hessian; these bounds will then be applicable as tight (since the bounds satisfy assumptions 1 and 2) pessimistic and optimistic models of the loss function in the neighborhood of some iterate θ_t:

Notation 6. Let $\theta_t \in \mathbb{R}^n$, $v_i \in \mathbb{R}^n$ an eigenvector of $\mathcal{H}(\theta_t)$.

$$M_t^i(x) \triangleq \nabla f(\theta_t)^\top v_i \cdot x + \frac{v_i^\top \mathcal{H}(\theta_t) v_i}{2} \cdot x^2 + \frac{L_t^i}{6} \cdot |x|^3 \tag{3}$$

$$m_t^i(x) \triangleq \nabla f(\theta_t)^\top v_i \cdot x + \frac{v_i^\top \mathcal{H}(\theta_t) v_i}{2} \cdot x^2 - \frac{L_t^i}{6} \cdot |x|^3 \tag{4}$$

Lemma 3.1. *Eigenspace Descent Bounds*

Let $f : \mathbb{R}^n \to \mathbb{R}$ be a function satisfying assumptions 1 and 2, and let $\theta_{t+1} \in \mathbb{R}^n$. Marking $\Delta\theta_t = \theta_{t+1} - \theta_t$, we have

$$\exists_{\left(L_t^i\right)_{i=1}^n \in (\mathbb{R}^+)^n} : f(\theta_{t+1}) - f(\theta_t) \leq \sum_{i=1}^n M_t^i\left(\Delta\theta_t^\top v_i\right) \tag{5}$$

$$\exists_{\left(L_t^i\right)_{i=1}^n \in (\mathbb{R}^+)^n} : f(\theta_{t+1}) - f(\theta_t) \geq \sum_{i=1}^n m_t^i\left(\Delta\theta_t^\top v_i\right) \tag{6}$$

We emphasize that unlike most previous works, our bound does not assume convexity and moreover it demonstrates the strong opportunity for descent in subspaces of the parameter space in which the loss function is concave, giving the first theoretical explanation for the experimental results of Alain et al. (2018) and Ghorbani et al. (2019), to the best of our knowledge (since the negative-definite Hessian corresponding to a locally concave loss function lowers the upper bound M_t^i of the per-iteration descent).

3.2 Exploiting these bounds for a minmax algorithm

Here we describe how to exploit the refined approximations that we obtain above to design a minimax optimal algorithm named `ELMO` which is depicted in Alg. 1.

To gain perspective on the upcoming algorithm as minmax-optimal, we restate a special case of the above lemma as follows: M_t^i is the pointwise maximal function satisfying assumptions 1 and 2:

$$M_t^i(x) = \max_{\substack{\tilde{f}:\mathbb{R}\to\mathbb{R} \\ \tilde{f}(\theta_t)=f(\theta_t)}} \tilde{f}\left(\theta_t + x \cdot v_i(\theta_t)\right)$$

In other words, M_t is the loss function (up to domain- and range-space translation) with the least opportunity for descent while still ensuring that all information collected by a second-order optimizer (with Hessian-Lipschitz oracle access) remains unchanged - i.e. *the adversarial loss function detailed in regret's definition*.

Since each element of the sum is a 1-dimensional trinomial, the minmax step is now easily obtained (due to orthogonality of the eigenspaces, resulting from the Hessian's symmetry) by taking the positive root of each term's derivative:

$$\Delta\theta_t^{*\top} v_i \triangleq \arg\min_{\Delta\theta_t} \sum_{i=1}^n M_t^i\left(\Delta\theta_t^\top v_i\right) = \frac{\sqrt{\lambda_i^2 + 2L_t^i\left|\nabla f(\theta_t)^\top v_i\right|} - \lambda_i}{L_t^i} \tag{7}$$

The above naturally induces a second-order training algorithm that we name Eigenspace-Lipschitz Minmax Optimizer (`ELMO`); which we describe in Alg. 1. We present a theoretical investigation of `ELMO` in Appendix C, and we leave its experimental evaluation to future work to maintain our focus on optimizer selection. We mark `EIGEN` an eigendecomposition subroutine and `LIPSCHITZ` a Lipschitz parameter oracle.

Algorithm 1 Algorithm `ELMO`

Require: $\epsilon \in \mathbb{R}^+, \theta_0 \in \mathbb{R}^n$, `EIGEN`, `LIPSCHITZ`
  $t \leftarrow 0$
  while $f(\theta_t) - f(\theta^*) > \epsilon$ **do**
    $(\lambda_i, v_i)_{i=1}^n \leftarrow \texttt{EIGEN}\left(\mathcal{H}(\theta_t)\right)$
    $\left(L_t^i\right)_{i=1}^n \leftarrow \texttt{LIPSCHITZ}\left(\theta_t, (v_i)_{i=1}^n\right)$
    $\left(\Delta\theta_t^i\right)_{i=1}^n \leftarrow \frac{\sqrt{\lambda_i^2 + 2L_t^i\left|\nabla f(\theta_t)^\top v_i\right|} - \lambda_i}{L_t^i}$
    $\theta_{t+1} \leftarrow \theta_t + \sum_{i=1}^n \Delta\theta_t^i \cdot v_i$
    $t \leftarrow t + 1$
  end while

Importantly, we observe equation 7's equal applicability to convex and concave regions of the domain space (and `ELMO` correspondingly) due to the lack of convexity assumptions. Indeed, `ELMO` makes use of concavity by taking larger steps in concave subspaces than otherwise (since `ELMO`'s second term's step size is proportional to $-\lambda_i$).

3.3 THE MINMAX PRECONDITIONER

Here we find algorithm ELMO's characteristic preconditioner. That is, we find Φ_t s.t. ELMO's step $\Delta\theta_t^*$ can be expressed as in definition 3. We begin by defining a metric of distance between optimization algorithms by the difference between the steps they take, and find the preconditioner matrix whose corresponding quasi-Newton algorithm is equivalent to algorithm ELMO.

Notation 7. For a given algorithm with step $\Delta\theta_t$ at iteration t, mark $\Delta\Delta^i\theta_t = \Delta\theta_t^\top v_i - \Delta\theta_t^{*\top} v_i$ the step's distance from ELMO's step. Since $\Delta\Delta^i\theta_t$ is a function of the algorithm chosen (through $\Delta\theta_t$), it is a function of that algorithm's defining preconditioner: $\Delta\Delta^i\theta_t = \Delta\Delta^i\theta_t(\Phi_t)$

This may be understood intuitively by noting that $\sum_{i=1}^n \Delta\Delta^i\theta_t$ is the L_1 norm of the difference between steps, as measured over the Hessian eigenbasis.

Lemma 3.2. *ELMO's preconditioner*

Let $f : \mathbb{R}^n \to \mathbb{R}$ satisfying assumptions 1 and 2. The preconditioner of the quasi-Newton algorithm that is equivalent to ELMO *(meaning $\left|\Delta\Delta^i\theta_t\right| = 0$) is*

$$\Phi_t^{\texttt{ELMO}} = \underset{\Phi_t \in \mathbb{R}^{n\times n}}{\arg\min} \left|\Delta\Delta^i\theta_t\left(\Phi_t\right)\right| = \left(\frac{\mathcal{H}\left(\theta_t\right) + \sqrt{\left(\mathcal{H}\left(\theta_t\right)\right)^2 + 2V \cdot diag\left(L_t^i \cdot \left|\nabla f\left(\theta_t\right)^\top v_i\right|\right)_{i=1}^n \cdot V^\top}}{2}\right)^{-1}$$

This preconditioner shows the mechanistic similarity of our algorithm to Newton's method: while Newton's method's preconditioner is simply the inverse Hessian (which may not be positive definite), the matrix whose inverse is our algorithm's preconditioner is an average between the Hessian and a positive definite, regularized version of the Hessian, whose every eigenvalue is no less than the corresponding Hessian eigenvalue's magnitude. This ensures positive semi-definiteness of our preconditioner, with regularization dependent on the loss function's rate of curvature shift.

In fact, Newton's algorithm (and correspondingly, most existing quasi-Newton algorithms that approximate it) may even lead to a worst-case *decrease* in model quality, even when the associated loss function is convex, for sufficiently great curvature shift (measured by Lipschitz parameter). Plugging Newton's step into equation 3 and rearranging tells us that $\forall_{i\in[n]s.t.\lambda_i\geq 0} : M_t^i\left(\frac{\left|\nabla f(\theta_t)_t v_i\right|}{\lambda_i}\right) \geq 0$ for any step t and eigenspace i with

$$L_t^i \geq 3\frac{\lambda_i^2}{\left|\nabla f\left(\theta_t\right)^\top v_i\right|} \tag{8}$$

3.4 DESCENT REGRET OF QUASI-NEWTON OPTIMIZATION ALGORITHMS

Algorithm ELMO is regret-optimal among first- and second-order methods in the sense that its model of the loss function is a generalization of quasi-Newton methods' and Gradient Descent's models (Appendix F), so it is natural to use it as a baseline against which to measure other optimizers' regret.

Different datasets imply different units for the parameters of neural networks, however (e.g. a neural network whose training dataset measures distances in miles will have differently scaled parameters than one whose distances are measured in kilometers, and different optimizer step sizes accordingly), so to maintain consistency across a variety of settings, we turn to dimensional analysis (Lin & Segel, 1988) to eliminate this effect on $\Delta\Delta^i\theta_t$. For simplicity, we restrict our discussion to the descent of the loss function's restriction to a given eigenspace *span* (v_i).

Notation 8. Mark $\Delta\Delta^i\theta_t' = \frac{\Delta\Delta^i\theta_t}{\Delta\theta_t^{*\top} v_i}$ the step's distance from ELMO's step relative to ELMO's step.

In fact, this optimizer metric generalizes several existing metrics, see Appendix D for details.

Theorem 3.3. *Worst-case descent rate for arbitrary optimizers*

Let $f : \mathbb{R}^n \to \mathbb{R}$ a twice-differentiable function satisfying assumptions 1 and 2, and let $\Delta\theta_t$ satisfy $M_t^i\left(\Delta\theta_t^\top v_i\right) \leq 0$. Then

$$\left|M_t^i\left(\Delta\theta_t^\top v_i\right)\right| = \Theta\left(1+\left|\Delta\Delta^i\theta_t'\right|^2\right)\cdot\left|M_t^i\left(\Delta\theta_t^{*\top} v_i\right)\right|$$

$$\left|m_t^i\left(\Delta\theta_t^\top v_i\right)\right| = \Theta\left(1+\left|\Delta\Delta^i\theta_t'\right|^p\right)\cdot\left|m_t^i\left(\Delta\theta_t^{*\top} v_i\right)\right| \tag{9}$$

$$\textit{with } p=\begin{cases}2 & \lambda_i>0\wedge\frac{\left|\nabla f(\theta_t)^\top v_i\right|}{\lambda_i^2}=0\\ 1 & else\end{cases}.$$

In other words, an arbitrary algorithm's descent regret (the ratio between the algorithm's descent in the adversarial setting and the optimal descent in the adversarial setting) is proportional to a polynomial of $\Delta\Delta^i\theta_t'$.

4 Dynamic optimizer selection

Here we describe a Meta-Optimizer which we name AMOS (Alg. 2) that dynamically combines different optimizers throughout the training process in order to boost performance. AMOS leans on our ELMO minimax optimal baseline.

The AMOS Meta-Optimizer In section 3.3 we saw a connection between the Lipschitz parameters and second-order optimizer applicability. In particular, we saw that large Lipschitz parameters are a counter-indication for second-order algorithms due to their indication that these algorithms poorly approximate the true loss function. This observation invites us to use these parameters to continually select between a computationally-heavy second-order algorithm and a computationally-light first-order algorithm for each training iteration to avoid the overhead of the second-order algorithm when its payoff does not warrant its overhead. Furthermore, we can combine these algorithms by partitioning the model parameters by the corresponding Lipschitz parameter magnitude, and assigning each partition to the appropriate optimizer.

Algorithm 2 Algorithm AMOS

Require: $\epsilon_1,\epsilon_2,L_{thresh},\alpha_L\in\mathbb{R}^+,\theta_0\in\mathbb{R}^n,I_{hess}\in 2^{\mathbb{N}},\texttt{OPT}^1,\texttt{OPT}^2$

1: $t\leftarrow 0$
2: **while** $f(\theta_t)-f(\theta_{t+1})>\epsilon_1$ **do**
3: **if** $t\in I_{hess}$ **then**
4: $(\lambda_i^t)_{i=1}^n\leftarrow\texttt{EIGEN}(\mathcal{H}(\theta_t))$
5: $\left(L_t^i\right)_{i=1}^n\leftarrow\alpha_L\cdot L_{t-1}^i+(1-\alpha_L)\cdot\frac{\left|\lambda_i^t-\lambda_i^{t-1}\right|}{\epsilon_2+\|\theta_t-\theta_{t-1}\|_2}$
6: **for** $i=1..n$ **do**
7: **if** $L_t^i>L_{thresh}$ **then**
8: $\texttt{OPTIM}_i\leftarrow\texttt{OPT}^1$
9: **else**
10: $\texttt{OPTIM}_i\leftarrow\texttt{OPT}^2$
11: **end if**
12: **end for**
13: **end if**
14: $(\Delta\theta_t)_i=\texttt{OPTIM}_i.\texttt{step}()$
15: $(\theta_{t+1})_i\leftarrow(\theta_t)_i+(\Delta\theta_t)_i$
16: $t\leftarrow t+1$
17: **end while**

Concretely, at each Hessian computation, Lipschitz parameters are approximated (line 5) as a running average of the slope of the Hessian eigenvalues, $L_t^i\approx\alpha_L L_{t-1}^i+(1-\alpha_L)\frac{|\lambda_i(x_t)-\lambda_i(x_{t-1})|}{\|x_t-x_{t-1}\|}$; model parameters[2] whose Lipschitz parameters are above a given threshold are assigned to the first-order optimizer until the next Hessian computation, while parameters whose Lipschitz parameters are beneath said threshold are assigned to the second-order optimizer (lines 7-10).

[2]Most popular second-order optimizers assume diagonal Hessian (e.g. Sophia) or block-diagonal Hessian (e.g. K-FAC) structure, the former of which associates each model parameter with its respective eigenvalue, allowing us to associate it with a Lipschitz parameter (and an analogous Lipschitz parameter may be associated with each block of model parameters in the latter case). For the remaining second-order optimizers, we partition model parameters into Hessian *eigenspaces*, and assign each eignspace to its respective optimizer, which reduces overhead by restricting the second-order optimizer to fewer eigenspaces, similarly to Sivan et al. (2024). See appendix A.

Figure 1: Training trajectory comparison. Our SGD-Sophia hybrid selection strategy outperforms all the rest while offloading responsibility for a significant portion of weights to SGD.

AMOS EXPERIMENTS

We tested AMOS[3] in the NanoGPT language modeling framework by Karpathy (2022); further details on settings in appendix K.

- We trained a 12-layer transformer with 12-head multihead attention on the TinyShakespeare dataset (Karpathy, 2015) for 2010 training iterations. This task involves modeling the character-level distribution of 40,000 lines taken from Shakespeare plays.
- Our baseline algorithm is AdamW with the tunedhyperparameters from vanilla NanoGPT.
- We use AMOS to adaptively select between SGD and Sophia throughout training.

Figure 1 presents the training trajectories from our experiments. We see that while pure SGD and Sophia are inferior to AdamW, by using AMOS we are able to combine SGD and Sophia to surpass AdamW on NanoGPT while also offloading 9% of the parameters on average (throughout training) and up to 91% (in a single iteration) to the cheaper first-order optimizer. We ascribe this additional loss minimization to our optimizer avoiding destructive Newton steps (as discussed in section 3.3).

5 LIPSCHITZ DISTRIBUTION

Previous works using the Hessian Lipschitz continuity assumption (e.g. ARC (Nesterov & Polyak, 2006) and its variants, O'Leary-Roseberry et al. (2019)) assume a single Lipschitz parameter for all eigenspaces. Although a finite number n of eigenspaces ensures that such a Lipschitz parameter exists (the maximal Lipschitz parameter), they fail to account for the distribution of these Lipschitz parameters over the eigenspaces. We claim that these parameters vary widely both over the eigenspaces and over the course of training, so that a single constant value fails to capture this structure; in this section we provide evidence for this claim. A discussion of sources of interest in this distribution is deferred to Appendix G.

The first source of evidence for our claim is from existing literature on the subject; we defer a discussion of this to appendix I. To test our claim directly, we modify an ARC implementation (Simpson & Wang, 2023) to compute the steps called for by ELMO at each point reached by a quasi-Newton algorithm, restricted to the subspace spanned by the eigenvectors corresponding to the single most positive and single most negative eigenvalues of each Hessian, and to use distinct Lipschitz parameters for each. Due to the computational difficulty of computing Lipschitz parameters precisely, we use these Lipschitz parameter values as an estimate for L^+, L^-. We note the crudeness of these adaptive measurements, merely adapting to keep $\frac{f(\theta_t)-f(\theta_{t+1})}{\left|\sum_{i=1}^{n} M_t^i\right|}$ within a given range with a restriction to powers of 2; nevertheless, the point is made.

A detailing of our experiment settings is given in appendix J as well as the full set of our experiment results, however we present two experiments in figure 2 for completeness. Our experiments show that

[3]AMOS: Adaptive Meta-algorithm for Optimizer Selection

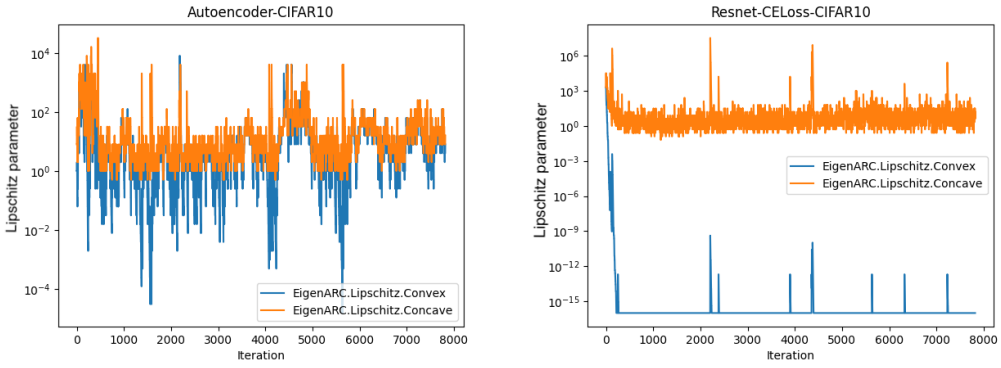

Figure 2: Comparisons of convex-subspace Lipschitz parameters to concave-subspace Lipschitz parameters. *Logarithmic scale*

as expected, $L^+ \ll L^-$, and the gap widens exponentially as training progresses in all cases except the autoencoders. Since we saw in section 3.3 that small convex Lipschitz parameters imply effective second-order optimization, this justifies common practice as noted by, e.g. O'Leary-Roseberry et al. (2019), of requiring the preconditioner to be an increasingly better approximation of the inverse Hessian (by increasing the strictness of the inverse Hessian approximation algorithm's stopping condition) as training progresses. Our findings also support Gur-Ari et al. (2018)'s observation that neural network optimization succeeds despite its nonconvexity due to the gradient residing primarily in convex subspaces, by demonstrating the stability of these convex subspaces.

Several factors seem to impact the size (by orders of magnitude) of the convex Lipschitz parameters, and they appear to be correlated with an intuitive sense of the difficulty of the setting being trained.

- The convex Lipschitz parameters are many orders of magnitude greater in the autoencoder task than in the classification task. We ascribe this gap to the more difficult task of learning a generative representation of the data instead of merely a discriminative representation of it (see Ng (2012, Chapter 4) for a discussion on generative vs. discriminative models).
- The convex Lipschitz parameters are reduced approximately 100x in the image classification task by adding residual connections. It is well known that residual connections reduce training difficulty (Li et al., 2018).
- The convex Lipschitz parameters are approximately 100x smaller when training ResNet to perform classification of natural images instead of Gaussian noise with random labels. We ascribe this to greater difficulty involved in discriminating noise, which requires partial memorization of the training set.

The Lipschitz parameters' indication of Newton's applicability suggests that the above observations may be applicable as a rule of thumb for optimizer selection; this is validated in experiments in Appendix E.

6 Conclusion

In this work we developed and analyzed a Hessian eigenspace Lipschitz-aware minmax optimization algorithm `ELMO` by taking an eigendecomposition-centric approach to locally modelling a loss function. We then proved a widely applicable worst-case relative descent rate bound for quasi-Newton optimizers by comparison to `ELMO`. We experimented with the Lipschitz distributions, discovering that they are correlated with task difficulty and that they are helpful for optimizer and optimization hyperparameters selection — specifically, integrating second-order information into optimizers at the cost of additional computational complexity is worthwhile in settings where the convex Lipschitz parameters are small, but not those where they are large. Finally, we used all of the above to design algorithm `AMOS` for dynamic optimizer selection, and demonstrated its performance in experiments.

REFERENCES

Naman Agarwal, Brian Bullins, Xinyi Chen, Elad Hazan, Karan Singh, Cyril Zhang, and Yi Zhang. Efficient full-matrix adaptive regularization. In Kamalika Chaudhuri and Ruslan Salakhutdinov (eds.), *Proceedings of the 36th International Conference on Machine Learning*, volume 97 of *Proceedings of Machine Learning Research*, pp. 102–110. PMLR, 09–15 Jun 2019. URL https://proceedings.mlr.press/v97/agarwal19b.html.

Naman Agarwal, Rohan Anil, Elad Hazan, Tomer Koren, and Cyril Zhang. Learning rate grafting: Transferability of optimizer tuning, 2022. URL https://openreview.net/forum?id=FpKgG31Z_i9.

Guillaume Alain, Nicolas Le Roux, and Pierre-Antoine Manzagol. Negative eigenvalues of the hessian in deep neural networks. In *6th International Conference on Learning Representations, ICLR 2018, Vancouver, BC, Canada, April 30 - May 3, 2018, Workshop Track Proceedings*. OpenReview.net, 2018. URL https://openreview.net/forum?id=S1iiddyDG.

Zeyuan Allen-Zhu. Katyusha: the first direct acceleration of stochastic gradient methods. *Proceedings of the 49th Annual ACM SIGACT Symposium on Theory of Computing*, 2016. URL https://api.semanticscholar.org/CorpusID:51918825.

Shun-ichi Amari. Natural Gradient Works Efficiently in Learning. *Neural Computation*, 10(2): 251–276, 02 1998. ISSN 0899-7667. doi: 10.1162/089976698300017746. URL https://doi.org/10.1162/089976698300017746.

Rohan Anil, Vineet Gupta, Tomer Koren, Kevin Regan, and Yoram Singer. Second order optimization made practical. *CoRR*, abs/2002.09018, 2020. URL https://arxiv.org/abs/2002.09018.

Somenath Bera and Vimal Shrivastava. Analysis of various optimizers on deep convolutional neural network model in the application of hyperspectral remote sensing image classification. *International Journal of Remote Sensing*, 41:2664–2683, 04 2020. doi: 10.1080/01431161.2019.1694725.

Dimitri P. Bertsekas. Incremental least squares methods and the extended kalman filter. *SIAM J. Optim.*, 6(3):807–822, 1996. doi: 10.1137/S1052623494268522. URL https://doi.org/10.1137/S1052623494268522.

Aleksandar Botev, Hippolyt Ritter, and David Barber. Practical Gauss-Newton optimisation for deep learning. In Doina Precup and Yee Whye Teh (eds.), *Proceedings of the 34th International Conference on Machine Learning*, volume 70 of *Proceedings of Machine Learning Research*, pp. 557–565. PMLR, 06–11 Aug 2017. URL https://proceedings.mlr.press/v70/botev17a.html.

Léon Bottou. Stochastic learning. In Olivier Bousquet, Ulrike von Luxburg, and Gunnar Rätsch (eds.), *Advanced Lectures on Machine Learning: ML Summer Schools 2003, Canberra, Australia, February 2 - 14, 2003, Tübingen, Germany, August 4 - 16, 2003, Revised Lectures*, pp. 146–168. Springer Berlin Heidelberg, Berlin, Heidelberg, 2004. ISBN 978-3-540-28650-9. doi: 10.1007/978-3-540-28650-9_7. URL https://doi.org/10.1007/978-3-540-28650-9_7.

Léon Bottou and Yann Lecun. On-line learning for very large datasets. *J. Applied Stochastic Models in Business and Industry*, 01 2004.

C. Cartis, N.I.M. Gould, and Ph.L. Toint. Complexity bounds for second-order optimality in unconstrained optimization. *Journal of Complexity*, 28(1):93–108, 2012a. ISSN 0885-064X. doi: https://doi.org/10.1016/j.jco.2011.06.001. URL https://www.sciencedirect.com/science/article/pii/S0885064X11000537.

Coralia Cartis, Nicholas I. M. Gould, and Philippe L. Toint. Adaptive cubic regularisation methods for unconstrained optimization. part i: motivation, convergence and numerical results. *Mathematical Programming*, 127(2):245–295, 2011a. doi: 10.1007/s10107-009-0286-5. URL https://doi.org/10.1007/s10107-009-0286-5.

Coralia Cartis, Nicholas I. M. Gould, and Philippe L. Toint. Adaptive cubic regularisation methods for unconstrained optimization. part ii: worst-case function- and derivative-evaluation complexity. *Mathematical Programming*, 130(2):295–319, 2011b. doi: 10.1007/s10107-009-0337-y. URL https://doi.org/10.1007/s10107-009-0337-y.

Coralia Cartis, Nicholas I. M. Gould, and Philippe L. Toint. Evaluation complexity of adaptive cubic regularization methods for convex unconstrained optimization. *Optimization Methods and Software*, 27:197 – 219, 2012b. URL https://api.semanticscholar.org/CorpusID:16647191.

Andrew R. Conn, Nicholas I. M. Gould, and Philippe L. Toint. *Trust-Region Methods*. SIAM, Philadelphia, PA, USA, 2000.

Yann N. Dauphin, Razvan Pascanu, Caglar Gulcehre, Kyunghyun Cho, Surya Ganguli, and Yoshua Bengio. Identifying and attacking the saddle point problem in high-dimensional non-convex optimization. In *Proceedings of the 27th International Conference on Neural Information Processing Systems - Volume 2*, NIPS'14, pp. 2933–2941, Cambridge, MA, USA, 2014. MIT Press.

Alexandre D'efossez, Léon Bottou, Francis R. Bach, and Nicolas Usunier. A simple convergence proof of adam and adagrad. *Trans. Mach. Learn. Res.*, 2022, 2020. URL https://api.semanticscholar.org/CorpusID:225213299.

Ron S. Dembo, Stanley C. Eisenstat, and Trond Steihaug. Inexact newton methods. *SIAM Journal on Numerical Analysis*, 19(2):400–408, 1982. doi: 10.1137/0719025. URL https://doi.org/10.1137/0719025.

J.E. Dennis and R.B. Schnabel. *Numerical Methods for Unconstrained Optimization and Nonlinear Equations*. Prentice-Hall Civil Engineering and Engineering Mechanics Se. Prentice-Hall, 1983. ISBN 9780136272168. URL https://books.google.co.il/books?id=4fFQAAAAMAAJ.

Tian Ding, Dawei Li, and Ruoyu Sun. Sub-optimal local minima exist for almost all over-parameterized neural networks. *ArXiv*, abs/1911.01413, 2019. URL https://api.semanticscholar.org/CorpusID:207870322.

John Duchi, Elad Hazan, and Yoram Singer. Adaptive subgradient methods for online learning and stochastic optimization. *Journal of Machine Learning Research*, 12(61):2121–2159, 2011a. URL http://jmlr.org/papers/v12/duchi11a.html.

John C. Duchi, Elad Hazan, and Yoram Singer. Adaptive subgradient methods for online learning and stochastic optimization. *J. Mach. Learn. Res.*, 12:2121–2159, 2011b. URL https://api.semanticscholar.org/CorpusID:538820.

S C Eisenstat and H F Walker. Choosing the forcing terms in an inexact newton method. *SIAM Journal on Scientific Computing*, 17(1), 1 1996. doi: 10.1137/0917003. URL https://www.osti.gov/biblio/218521.

William R. Esposito and Christodoulos A. Floudas. Gauss–newton method: Least squares, relation to newton's methodgauss–newton method: Least squares, relation to newton's method. In Christodoulos A. Floudas and Panos M. Pardalos (eds.), *Encyclopedia of Optimization*, pp. 733–738. Springer US, Boston, MA, 2001. ISBN 978-0-306-48332-5. doi: 10.1007/0-306-48332-7_151. URL https://doi.org/10.1007/0-306-48332-7_151.

Reuben Feinman. Pytorch-minimize: a library for numerical optimization with autograd, 2021. URL https://github.com/rfeinman/pytorch-minimize.

Dan Garber, Elad Hazan, Chi Jin, Kakade Sham, Cameron Musco, Praneeth Netrapalli, and Aaron Sidford. Faster eigenvector computation via shift-and-invert preconditioning. In Maria Florina Balcan and Kilian Q. Weinberger (eds.), *Proceedings of The 33rd International Conference on Machine Learning*, volume 48 of *Proceedings of Machine Learning Research*, pp. 2626–2634, New York, New York, USA, 20–22 Jun 2016. PMLR. URL https://proceedings.mlr.press/v48/garber16.html.

R. Garmanjani. A note on the worst-case complexity of nonlinear stepsize control methods for convex smooth unconstrained optimization. *Optimization*, 71:1–11, 10 2020. doi: 10.1080/02331934.2020.1830088.

Rong Ge, Furong Huang, Chi Jin, and Yang Yuan. Escaping from saddle points — online stochastic gradient for tensor decomposition. In Peter Grünwald, Elad Hazan, and Satyen Kale (eds.), *Proceedings of The 28th Conference on Learning Theory*, volume 40 of *Proceedings of Machine Learning Research*, pp. 797–842, Paris, France, 03–06 Jul 2015. PMLR. URL https://proceedings.mlr.press/v40/Ge15.html.

Behrooz Ghorbani, Shankar Krishnan, and Ying Xiao. An investigation into neural net optimization via hessian eigenvalue density. In Kamalika Chaudhuri and Ruslan Salakhutdinov (eds.), *Proceedings of the 36th International Conference on Machine Learning*, volume 97 of *Proceedings of Machine Learning Research*, pp. 2232–2241. PMLR, 09–15 Jun 2019. URL https://proceedings.mlr.press/v97/ghorbani19b.html.

Donald Goldfarb, Yi Ren, and Achraf Bahamou. Practical quasi-newton methods for training deep neural networks. In H. Larochelle, M. Ranzato, R. Hadsell, M.F. Balcan, and H. Lin (eds.), *Advances in Neural Information Processing Systems*, volume 33, pp. 2386–2396. Curran Associates, Inc., 2020. URL https://proceedings.neurips.cc/paper_files/paper/2020/file/192fc044e74dffea144f9ac5dc9f3395-Paper.pdf.

I. J. Good. Rational decisions. *Journal of the Royal Statistical Society. Series B (Methodological)*, 14 (1):107–114, 1952. ISSN 00359246. URL http://www.jstor.org/stable/2984087.

Andreas Griewank. The modification of newton's method for unconstrained optimization by bounding cubic terms. Technical report, Department of Applied Mathematics and Theoretical Physics, University of Cambridge, United Kingdom, 1981.

Vineet Gupta, Tomer Koren, and Yoram Singer. Shampoo: Preconditioned stochastic tensor optimization. In Jennifer Dy and Andreas Krause (eds.), *Proceedings of the 35th International Conference on Machine Learning*, volume 80 of *Proceedings of Machine Learning Research*, pp. 1842–1850. PMLR, 10–15 Jul 2018. URL https://proceedings.mlr.press/v80/gupta18a.html.

Guy Gur-Ari, Daniel A. Roberts, and Ethan Dyer. Gradient descent happens in a tiny subspace. *ArXiv*, abs/1812.04754, 2018. URL https://api.semanticscholar.org/CorpusID:54480858.

Kaiming He, X. Zhang, Shaoqing Ren, and Jian Sun. Deep residual learning for image recognition. *2016 IEEE Conference on Computer Vision and Pattern Recognition (CVPR)*, pp. 770–778, 2015. URL https://api.semanticscholar.org/CorpusID:206594692.

M.F. Hutchinson. A stochastic estimator of the trace of the influence matrix for laplacian smoothing splines. *Communication in Statistics- Simulation and Computation*, 18:1059–1076, 01 1989. doi: 10.1080/03610919008812866.

Maarten Jansen and Gerda Claeskens. Cramér–rao inequality. In Miodrag Lovric (ed.), *International Encyclopedia of Statistical Science*, pp. 322–323. Springer Berlin Heidelberg, Berlin, Heidelberg, 2011. ISBN 978-3-642-04898-2. doi: 10.1007/978-3-642-04898-2_197. URL https://doi.org/10.1007/978-3-642-04898-2_197.

Chi Jin, Rong Ge, Praneeth Netrapalli, Sham M. Kakade, and Michael I. Jordan. How to escape saddle points efficiently. In Doina Precup and Yee Whye Teh (eds.), *Proceedings of the 34th International Conference on Machine Learning*, volume 70 of *Proceedings of Machine Learning Research*, pp. 1724–1732. PMLR, 06–11 Aug 2017. URL https://proceedings.mlr.press/v70/jin17a.html.

Andrej Karpathy. char-rnn. https://github.com/karpathy/char-rnn, 2015.

Andrej Karpathy. NanoGPT. https://github.com/karpathy/nanoGPT, 2022.

Kenji Kawaguchi. Deep learning without poor local minima. In D. Lee, M. Sugiyama, U. Luxburg, I. Guyon, and R. Garnett (eds.), *Advances in Neural Information Processing Systems*, volume 29. Curran Associates, Inc., 2016. URL https://proceedings.neurips.cc/paper_files/paper/2016/file/f2fc990265c712c49d51a18a32b39f0c-Paper.pdf.

Kenji Kawaguchi and Yoshua Bengio. Depth with nonlinearity creates no bad local minima in resnets. *Neural Networks*, 118:167–174, 2019. ISSN 0893-6080. doi: https://doi.org/10.1016/j.neunet.2019.06.009. URL https://www.sciencedirect.com/science/article/pii/S0893608019301820.

Diederik Kingma and Jimmy Ba. Adam: A method for stochastic optimization. *arXiv preprint arXiv:1412.6980*, 2014.

Yann LeCun. *PhD thesis: Modeles connexionnistes de l'apprentissage (connectionist learning models)*. PhD thesis, Université Pierre et Marie Curie, Paris, France, 1987. URL https://api.semanticscholar.org/CorpusID:151887454.

Kfir Yehuda Levy. The power of normalization: Faster evasion of saddle points. *ArXiv*, abs/1611.04831, 2016. URL https://api.semanticscholar.org/CorpusID:16706102.

Hao Li, Zheng Xu, Gavin Taylor, Christoph Studer, and Tom Goldstein. Visualizing the loss landscape of neural nets. In S. Bengio, H. Wallach, H. Larochelle, K. Grauman, N. Cesa-Bianchi, and R. Garnett (eds.), *Advances in Neural Information Processing Systems*, volume 31. Curran Associates, Inc., 2018. URL https://proceedings.neurips.cc/paper_files/paper/2018/file/a41b3bb3e6b050b6c9067c67f663b915-Paper.pdf.

Lin and Segel. *Mathematics Applied to Deterministic Problems in the Natural Sciences*. SIAM, Philadelphia, 1988. ISBN 978-0-89871-229-2. doi: 10.1137/1.9781611971347. URL https://doi.org/10.1137/1.9781611971347.

Hong Liu, Zhiyuan Li, David Leo Wright Hall, Percy Liang, and Tengyu Ma. Sophia: A scalable stochastic second-order optimizer for language model pre-training. In *The Twelfth International Conference on Learning Representations*, 2024. URL https://openreview.net/forum?id=3xHDeA8Noi.

Kenneth L. Manders and Leonard Adleman. Np-complete decision problems for binary quadratics. *Journal of Computer and System Sciences*, 16(2):168–184, 1978. ISSN 0022-0000. doi: https://doi.org/10.1016/0022-0000(78)90044-2. URL https://www.sciencedirect.com/science/article/pii/0022000078900442.

James Martens. Deep learning via hessian-free optimization. In Johannes Fürnkranz and Thorsten Joachims (eds.), *ICML*, pp. 735–742. Omnipress, 2010. URL http://dblp.uni-trier.de/db/conf/icml/icml2010.html#Martens10.

James Martens. New insights and perspectives on the natural gradient method. *J. Mach. Learn. Res.*, 21(1), jan 2020. ISSN 1532-4435.

James Martens and Roger Grosse. Optimizing neural networks with kronecker-factored approximate curvature. In Francis Bach and David Blei (eds.), *Proceedings of the 32nd International Conference on Machine Learning*, volume 37 of *Proceedings of Machine Learning Research*, pp. 2408–2417, Lille, France, 07–09 Jul 2015. PMLR. URL https://proceedings.mlr.press/v37/martens15.html.

Harshal Mittal, Kartikey Pandey, and Yash Kant. Iclr reproducibility challenge report (padam : Closing the generalization gap of adaptive gradient methods in training deep neural networks). *ArXiv*, abs/1901.09517, 2019. URL https://api.semanticscholar.org/CorpusID:249647677.

Aatila Mustapha, Lachgar Mohamed, and Kartit Ali. Comparative study of optimization techniques in deep learning: Application in the ophthalmology field. *Journal of Physics: Conference Series*, 1743, 2021. URL https://api.semanticscholar.org/CorpusID:234179873.

Yurii Nesterov and B. T. Polyak. Cubic regularization of newton method and its global performance. *Mathematical Programming*, 108(1):177–205, 2006. doi: 10.1007/s10107-006-0706-8. URL https://doi.org/10.1007/s10107-006-0706-8.

Andrew Ng. Cs229 lecture notes - supervised learning. Available at https://cs229.stanford.edu/lectures-spring2022/main_notes.pdf, 2012.

Quynh Nguyen, Mahesh Chandra Mukkamala, and Matthias Hein. On the loss landscape of a class of deep neural networks with no bad local valleys. In *International Conference on Learning Representations*, 2019. URL https://openreview.net/forum?id=HJgXsjA5tQ.

Jorge Nocedal and Stephen J. Wright. *Numerical Optimization*. Springer, New York, NY, USA, 2e edition, 2006.

Thomas O'Leary-Roseberry, Nick Alger, and Omar Ghattas. Inexact newton methods for stochastic non-convex optimization with applications to neural network training. *arXiv: Optimization and Control*, 2019. URL https://api.semanticscholar.org/CorpusID:155100112.

P.J. Olver and C. Shakiban. *Applied Linear Algebra*. Prentice Hall, 2006. ISBN 9780131473829. URL https://books.google.co.il/books?id=D2tyQgAACAAJ.

OpenAI, Josh Achiam, Steven Adler, Sandhini Agarwal, Lama Ahmad, Ilge Akkaya, Florencia Leoni Aleman, Diogo Almeida, Janko Altenschmidt, Sam Altman, Shyamal Anadkat, Red Avila, Igor Babuschkin, Suchir Balaji, Valerie Balcom, Paul Baltescu, Haiming Bao, Mohammad Bavarian, Jeff Belgum, Irwan Bello, Jake Berdine, Gabriel Bernadett-Shapiro, Christopher Berner, Lenny Bogdonoff, Oleg Boiko, Madelaine Boyd, Anna-Luisa Brakman, Greg Brockman, Tim Brooks, Miles Brundage, Kevin Button, Trevor Cai, Rosie Campbell, Andrew Cann, Brittany Carey, Chelsea Carlson, Rory Carmichael, Brooke Chan, Che Chang, Fotis Chantzis, Derek Chen, Sully Chen, Ruby Chen, Jason Chen, Mark Chen, Ben Chess, Chester Cho, Casey Chu, Hyung Won Chung, Dave Cummings, Jeremiah Currier, Yunxing Dai, Cory Decareaux, Thomas Degry, Noah Deutsch, Damien Deville, Arka Dhar, David Dohan, Steve Dowling, Sheila Dunning, Adrien Ecoffet, Atty Eleti, Tyna Eloundou, David Farhi, Liam Fedus, Niko Felix, Simón Posada Fishman, Juston Forte, Isabella Fulford, Leo Gao, Elie Georges, Christian Gibson, Vik Goel, Tarun Gogineni, Gabriel Goh, Rapha Gontijo-Lopes, Jonathan Gordon, Morgan Grafstein, Scott Gray, Ryan Greene, Joshua Gross, Shixiang Shane Gu, Yufei Guo, Chris Hallacy, Jesse Han, Jeff Harris, Yuchen He, Mike Heaton, Johannes Heidecke, Chris Hesse, Alan Hickey, Wade Hickey, Peter Hoeschele, Brandon Houghton, Kenny Hsu, Shengli Hu, Xin Hu, Joost Huizinga, Shantanu Jain, Shawn Jain, Joanne Jang, Angela Jiang, Roger Jiang, Haozhun Jin, Denny Jin, Shino Jomoto, Billie Jonn, Heewoo Jun, Tomer Kaftan, Łukasz Kaiser, Ali Kamali, Ingmar Kanitscheider, Nitish Shirish Keskar, Tabarak Khan, Logan Kilpatrick, Jong Wook Kim, Christina Kim, Yongjik Kim, Jan Hendrik Kirchner, Jamie Kiros, Matt Knight, Daniel Kokotajlo, Łukasz Kondraciuk, Andrew Kondrich, Aris Konstantinidis, Kyle Kosic, Gretchen Krueger, Vishal Kuo, Michael Lampe, Ikai Lan, Teddy Lee, Jan Leike, Jade Leung, Daniel Levy, Chak Ming Li, Rachel Lim, Molly Lin, Stephanie Lin, Mateusz Litwin, Theresa Lopez, Ryan Lowe, Patricia Lue, Anna Makanju, Kim Malfacini, Sam Manning, Todor Markov, Yaniv Markovski, Bianca Martin, Katie Mayer, Andrew Mayne, Bob McGrew, Scott Mayer McKinney, Christine McLeavey, Paul McMillan, Jake McNeil, David Medina, Aalok Mehta, Jacob Menick, Luke Metz, Andrey Mishchenko, Pamela Mishkin, Vinnie Monaco, Evan Morikawa, Daniel Mossing, Tong Mu, Mira Murati, Oleg Murk, David Mély, Ashvin Nair, Reiichiro Nakano, Rajeev Nayak, Arvind Neelakantan, Richard Ngo, Hyeonwoo Noh, Long Ouyang, Cullen O'Keefe, Jakub Pachocki, Alex Paino, Joe Palermo, Ashley Pantuliano, Giambattista Parascandolo, Joel Parish, Emy Parparita, Alex Passos, Mikhail Pavlov, Andrew Peng, Adam Perelman, Filipe de Avila Belbute Peres, Michael Petrov, Henrique Ponde de Oliveira Pinto, Michael, Pokorny, Michelle Pokrass, Vitchyr H. Pong, Tolly Powell, Alethea Power, Boris Power, Elizabeth Proehl, Raul Puri, Alec Radford, Jack Rae, Aditya Ramesh, Cameron Raymond, Francis Real, Kendra Rimbach, Carl Ross, Bob Rotsted, Henri Roussez, Nick Ryder, Mario Saltarelli, Ted Sanders, Shibani Santurkar, Girish Sastry, Heather Schmidt, David Schnurr, John Schulman, Daniel Selsam, Kyla Sheppard, Toki Sherbakov, Jessica Shieh, Sarah Shoker, Pranav Shyam, Szymon Sidor, Eric Sigler, Maddie Simens, Jordan Sitkin, Katarina Slama, Ian Sohl, Benjamin Sokolowsky, Yang Song, Natalie Staudacher, Felipe Petroski Such, Natalie Summers, Ilya Sutskever, Jie Tang, Nikolas Tezak, Madeleine B. Thompson, Phil Tillet, Amin Tootoonchian, Elizabeth Tseng, Preston Tuggle, Nick Turley, Jerry Tworek, Juan Felipe Cerón Uribe, Andrea Vallone, Arun Vijayvergiya,

Chelsea Voss, Carroll Wainwright, Justin Jay Wang, Alvin Wang, Ben Wang, Jonathan Ward, Jason Wei, CJ Weinmann, Akila Welihinda, Peter Welinder, Jiayi Weng, Lilian Weng, Matt Wiethoff, Dave Willner, Clemens Winter, Samuel Wolrich, Hannah Wong, Lauren Workman, Sherwin Wu, Jeff Wu, Michael Wu, Kai Xiao, Tao Xu, Sarah Yoo, Kevin Yu, Qiming Yuan, Wojciech Zaremba, Rowan Zellers, Chong Zhang, Marvin Zhang, Shengjia Zhao, Tianhao Zheng, Juntang Zhuang, William Zhuk, and Barret Zoph. Gpt-4 technical report, 2024.

Panos M. Pardalos and Stephen A. Vavasis. Quadratic programming with one negative eigenvalue is np-hard. *Journal of Global Optimization*, 1(1):15–22, 1991. doi: 10.1007/BF00120662. URL https://doi.org/10.1007/BF00120662.

Dylan Patel and Gerald Wong. Gpt-4 architecture, infrastructure, training dataset, costs, vision, moe. https://www.semianalysis.com/p/gpt-4-architecture-infrastructure, 2023. Accessed: 2024-05-01.

Barak A. Pearlmutter. Fast Exact Multiplication by the Hessian. *Neural Computation*, 6(1):147–160, 01 1994. ISSN 0899-7667. doi: 10.1162/neco.1994.6.1.147. URL https://doi.org/10.1162/neco.1994.6.1.147.

Karl Pearson. Note on Regression and Inheritance in the Case of Two Parents. *Proceedings of the Royal Society of London Series I*, 58:240–242, January 1895.

Sebastian Ruder. An overview of gradient descent optimization algorithms. *ArXiv*, abs/1609.04747, 2016. URL https://api.semanticscholar.org/CorpusID:17485266.

Levent Sagun, Léon Bottou, and Yann LeCun. Eigenvalues of the hessian in deep learning: Singularity and beyond. *arXiv: Learning*, 2016. URL https://api.semanticscholar.org/CorpusID:35723845.

Robin M Schmidt, Frank Schneider, and Philipp Hennig. Descending through a crowded valley - benchmarking deep learning optimizers. In Marina Meila and Tong Zhang (eds.), *Proceedings of the 38th International Conference on Machine Learning*, volume 139 of *Proceedings of Machine Learning Research*, pp. 9367–9376. PMLR, 18–24 Jul 2021. URL https://proceedings.mlr.press/v139/schmidt21a.html.

Nicol Schraudolph. Fast curvature matrix-vector products for second-order gradient descent. *Neural computation*, 14:1723–38, 08 2002. doi: 10.1162/08997660260028683.

Cooper Simpson and Jaden Wang. PyTorch-ARC. github.com/RS-Coop/PyTorch-ARC, 2023. Adaptive Regularization with Cubics (ARC) optimizer for PyTorch.

Hadar Sivan, Moshe Gabel, and Assaf Schuster. FOSI: Hybrid first and second order optimization. In *The Twelfth International Conference on Learning Representations*, 2024. URL https://openreview.net/forum?id=NvbeD9Ttkx.

Daniel Soudry and Yair Carmon. No bad local minima: Data independent training error guarantees for multilayer neural networks. *ArXiv*, abs/1605.08361, 2016. URL https://api.semanticscholar.org/CorpusID:3029264.

Tijmen Tieleman and Geoffrey Hinton. Lecture 6.5-rmsprop: Divide the gradient by a running average of its recent magnitude. *COURSERA: Neural networks for machine learning*, 4(2):26–31, 2012.

Philippe L. Toint. Nonlinear stepsize control, trust regions and regularizations for unconstrained optimization. *Optimization Methods and Software*, 28(1):82–95, 2013. doi: 10.1080/10556788.2011.610458. URL https://doi.org/10.1080/10556788.2011.610458.

J.F. Traub. *Iterative Methods for the Solution of Equations*. AMS Chelsea Publishing Series. Chelsea, 1982. ISBN 9780828403122. URL https://books.google.co.il/books?id=se3YdgFgz4YC.

Sharan Vaswani, Reza Babanezhad, Jose Gallego, Aaron Mishkin, Simon Lacoste-Julien, and Nicolas Le Roux. To each optimizer a norm, to each norm its generalization. *ArXiv*, abs/2006.06821, 2020. URL https://api.semanticscholar.org/CorpusID:219636073.

Neha Wadia, Daniel Duckworth, Samuel S Schoenholz, Ethan Dyer, and Jascha Sohl-Dickstein. Whitening and second order optimization both make information in the dataset unusable during training, and can reduce or prevent generalization. In Marina Meila and Tong Zhang (eds.), *Proceedings of the 38th International Conference on Machine Learning*, volume 139 of *Proceedings of Machine Learning Research*, pp. 10617–10629. PMLR, 18–24 Jul 2021. URL https://proceedings.mlr.press/v139/wadia21a.html.

Xiao Wang, Shiqian Ma, Donald Goldfarb, and Wei Liu. Stochastic quasi-newton methods for nonconvex stochastic optimization. *SIAM Journal on Optimization*, 27, 07 2016. doi: 10.1137/15M1053141.

Rachel Ward, Xiaoxia Wu, and Leon Bottou. AdaGrad stepsizes: Sharp convergence over nonconvex landscapes. In Kamalika Chaudhuri and Ruslan Salakhutdinov (eds.), *Proceedings of the 36th International Conference on Machine Learning*, volume 97 of *Proceedings of Machine Learning Research*, pp. 6677–6686. PMLR, 09–15 Jun 2019. URL https://proceedings.mlr.press/v97/ward19a.html.

Peng Xu, Farbod Roosta-Khorasan, and Michael Mahoney. Second-order optimization for non-convex machine learning: An empirical study. In *Proceedings of the 2020 SIAM International Conference on Data Mining*, 08 2017.

Peng Xu, Fred Roosta, and Michael W. Mahoney. Newton-type methods for non-convex optimization under inexact hessian information. *Mathematical Programming*, 184(1):35–70, 2020. doi: 10.1007/s10107-019-01405-z. URL https://doi.org/10.1007/s10107-019-01405-z.

Robert M. Young. 75.9 euler's constant. *The Mathematical Gazette*, 75(472):187–190, 1991. ISSN 00255572. URL http://www.jstor.org/stable/3620251.

Xiao-Hu Yu and Guo-An Chen. On the local minima free condition of backpropagation learning. *IEEE Transactions on Neural Networks*, 6(5):1300–1303, 1995. doi: 10.1109/72.410380.

Matthew D. Zeiler. Adadelta: An adaptive learning rate method. *ArXiv*, abs/1212.5701, 2012. URL https://api.semanticscholar.org/CorpusID:7365802.

Pan Zhou, Jiashi Feng, Chao Ma, Caiming Xiong, Steven Chu Hong Hoi, and Weinan E. Towards theoretically understanding why sgd generalizes better than adam in deep learning. In H. Larochelle, M. Ranzato, R. Hadsell, M.F. Balcan, and H. Lin (eds.), *Advances in Neural Information Processing Systems*, volume 33, pp. 21285–21296. Curran Associates, Inc., 2020. URL https://proceedings.neurips.cc/paper_files/paper/2020/file/f3f27a324736617f20abbf2ffd806f6d-Paper.pdf.

Milija Županski. A preconditioning algorithm for large-scale minimization problems. *Tellus A: Dynamic Meteorology and Oceanography*, Jan 1993. doi: 10.3402/tellusa.v45i5.15048.

A Quasi-Newton Challenges and Proposed Solutions

Notation 9. Let $A \in \mathbb{R}^{n\times n}$. We mark $\lambda_{\min}(A), \lambda_{\max}(A)$ the minimal/maximal eigenvalue of A, respectively, and their ratio $\kappa(A) = \frac{\lambda_{\max}(A)}{\lambda_{\min}(A)}$ the condition number of A.

Some of the challenges involved in training neural networks include:

- Because the models and data often have very complex structures, obtaining precisely optimal parameters is often computationally prohibitive. As a result, one must satisfy oneself with a small degree of suboptimality in the model's parameters, chosen to be small enough to satisfy one's needs while not exhausting the computational capacity at hand.
- Since many model architectures (e.g. artificial neural networks) have very complex structures, the loss function is generallhy non-convex as a function of the model's parameters. This makes finding the globally optimal choice of parameters an NP-hard problem (Pardalos & Vavasis, 1991; Manders & Adleman, 1978). As a result, one must satisfy oneself with merely a local minimum of the loss function (that is, a point at which the norm of the gradient

w.r.t. the model parameters is zero, and the function is locally convex, or equivalently, the Hessian is positive semi-definite). This is often considered sufficient (see Soudry & Carmon (2016); Kawaguchi & Bengio (2019); Kawaguchi (2016); Nguyen et al. (2019)), however this does not apply to saddle points and local maxima (points at which the gradient norm is zero but the Hessian is not positive definite). Although some work has been done on trying to eliminate this problem by eliminating local- but not global- minima via overparameterization (Yu & Chen, 1995), further work (Ding et al., 2019) has shown that this does not scale to deep neural networks.

- As mentioned previously, there is no single universally optimal optimizer, even among existing optimizers.

As a result, sophisticated optimizers are necessary to contend with different neural network training scenarios. Restricting ourselves to quasi-newton optimization algorithms, scenarios with $n \gg 0$ (a common theme in machine learning, where n may be in the millions, billions, or even trillions, as GPT4 (OpenAI et al., 2024) is rumored to have. See Patel & Wong (2023)) are that computing and inverting the Hessian (with respective complexities $\mathcal{O}\left(n^2\right), \mathcal{O}\left(n^3\right)$) may be computationally prohibitive. Also, one must ensure that

$$\Phi_t \succeq 0 \tag{10}$$

to ensure that $\theta_{t+1} - \theta_t$ is a descent direction of f. This is because $-\nabla f\left(\theta_t\right)$ is a descent direction of f, which implies that for all $v \in \mathbb{R}^n$, $-\alpha \cdot \nabla f\left(\theta_t\right)^\top v \cdot v^\top$ is a descent direction for $\alpha > 0$ and an ascent direction for $\alpha < 0$. However, if (λ_i, v_i) is an eigenvalue-eigenvector pair of Φ_t with $\lambda_i < 0$ then $-v_i^\top \cdot \Phi_t \nabla f\left(\theta_t\right) \cdot v_i = -\lambda_i \nabla f\left(\theta_t\right)^\top \cdot v_i \cdot v_i$ which is an ascent direction, and then a better preconditioner could immediately be obtained by taking $\tilde{\Phi}_t$ with eigenpairs $\left(\tilde{\lambda_j}, \tilde{v_j}\right), \tilde{v_j} = v_j, \tilde{\lambda_j} = \begin{cases} \lambda_j & j \neq i \\ 0 & j = i \end{cases}$ to prevent an ascent in the subspace (a.k.a. eigenspace) *span*(v_i).

Three common ways to contend with these challenges are:

- **The Hessian-Free approach** Making use of Pearlmutter (1994) to compute Hessian-vector products without explicit computation of the Hessian, one uses conjugate-gradient (Olver & Shakiban, 2006) iterations to compute progressively finer approximations to $\left(\mathcal{H}\left(\theta_t\right)\right)^{-1} \cdot \nabla f\left(\theta_t\right)$, stopping when one reaches a dimension with negative curvature. See, for instance, Martens (2010).
- **The Lanczos eigendecomposition approach** Making use of Lanczos iterations (Olver & Shakiban, 2006), one decomposes the Hessian into its eigendecomposition, and explicitly edits its eigenvalues. See, for instance, Dauphin et al. (2014); Sivan et al. (2024).
- **The Gauss-Newton approach** Using the generalized Gauss-Newton approximation to the Hessian (Esposito & Floudas, 2001; Schraudolph, 2002), one can obtain a matrix which has the following good properties:
  - Well approximated by a Kronecker product (sparse representation), which allows one to represent it and multiply by it very cheaply
  - Positive semi-definite
  - Can be computed with only a first-order loss function gradient oracle
  - Well approximates the true loss Hessian, when the second derivative of the model or the residual loss $\left(f\left(\theta_t\right) - f\left(\theta^*\right)\right)$ is insignificant next to the generalized Gauss Newton

  Some examples of this approach include Agarwal et al. (2019); Botev et al. (2017); Gupta et al. (2018); Martens & Grosse (2015); Goldfarb et al. (2020); Anil et al. (2020). Of particular note are examples that make diagonal approximations to the Gauss-Newton, as noted by Martens (2020), that are most often viewed as first-order methods, such as Adagrad (Duchi et al., 2011a), RMSProp (Tieleman & Hinton, 2012), and Adam (Kingma & Ba, 2014). As noted by Martens (2020), due to the strong connection between the generalized Gauss-Newton and the Fischer Information matrix (when the loss function is cross-entropy loss (Good, 1952)), one can achieve certain theoretical benefits when using such methods, such as Fischer efficiency; see Amari (1998) for instance, which views θ_t as an unbiased estimator of θ^* of f, and uses the Cramer-Rao inequality (Jansen & Claeskens, 2011) to

lower-bound the minimal number of iterations required to minimize the variance of said estimator as a function of the Fischer Information due to the number of samples consumed by each iteration.

See Nocedal & Wright (2006, Chapters 3.3,3.4) for further discussion of these approaches.

In order for a minimization problem to be well-defined, one must assume that f is lower-bounded. We can infer from this that any subset of the domain space in which f is concave must be a bounded set (because nonconstant concave functions with unbounded domains are not lower-bounded); this means that the second-order Taylor approximation of the function must have a bounded neighborhood in which it approximates the function well. Additionally, even in subsets of the domain space in which f is convex, the neighborhood in which the second-order Taylor approximation of the loss function well-approximates the true loss function may be bounded. To address this, two common approaches been proposed in the literature, namely:

- **The Trust Regions Approach**, which explicitly maintains a radius of the neighborhood in which the second-order Taylor polynomial is a good approximation of the function, and bounds the step size to that radius. See Conn et al. (2000), Nocedal & Wright (2006, Chapter 4).
- **The Cubic Regularization Approach**, which assumes that Hessian is Lipschitz continuous (using the L2 vector-induced matrix norm to measure distances between Hessians), and as such can upper bound the distance between two points of the function using a third-order polynomial (discussed below, see Lemma 4.1.14 from Dennis & Schnabel (1983)). See Nesterov & Polyak (2006) for an algorithm based on this approach that adaptively estimates the Hessian-Lipschitz parameter.

B Other convergence rate measures

Convergence rates to first-order criticality Most works on convergence rates in the non-convex regime bound the number of iterations necessary to achieve first-order criticality ($\left\|\nabla f\left(\theta_t\right)\right\|_2 = 0$) by means of finding an ϵ_g-stationary point (a point at which $\left\|\nabla f\left(\theta_t\right)\right\|_2 \leq \epsilon_g$). The seminal work Wang et al. (2016) provide a convergence rate bound for general optimizers (with very weak assumptions) in the non-convex regime of $\mathcal{O}\left(\kappa^{\frac{2}{1-\nu}}\left(\Phi_t\right) \cdot \epsilon_g^{-\frac{1}{1-\nu}}\right)$ with learning rate $\alpha_t = \mathcal{O}\left(t^{-\nu}\right)$ and $\nu \in (0.5, 1)$. However, this bound is minimized by setting Φ_t to the minimizer of $\kappa\left(\Phi_t\right)$, which is a scalar matrix; this is equivalent to gradient descent, a first-order method. Experiments (see Sivan et al. (2024), for instance) and theory show that higher-order methods can achieve faster rates of convergence in our setting, demonstrating looseness of this convergence rate bound. See also D'efossez et al. (2020) who give such convergence rate bounds (requiring t iterations, for t s.t. $\frac{\sqrt{t}}{\log(t)} = \Omega\left(\epsilon_g^{-1}\right)$) for Adam and Adagrad, and Ward et al. (2019) who give such convergence rate bounds (at $\mathcal{O}\left(\epsilon_g^{-1}\right)$) for gradient descent with Adagrad-grafted step-sizes (see Agarwal et al. (2022) for a discussion on learning rate grafting).

Convergence rates to second-order criticality A few go further in bounding the number of steps required to achieve second-order criticality (a point satisfying $\left\|\nabla f\left(\theta_t\right)\right\|_2 < \epsilon_g, -\lambda_{\min}\left(\mathcal{H}\left(\theta_t\right)\right) < \epsilon_H$). For instance, Nesterov & Polyak (2006); Cartis et al. (2011b); Xu et al. (2020) provide such bounds (at $\mathcal{O}\left(\max(\epsilon_g, \epsilon_H)^{-3}\right)$) on variants of the ARC algorithm, and Levy (2016); Jin et al. (2017); Ge et al. (2015) provide such bounds for varieties of SGD. This is of great importance since as noted, local minima are generally considered sufficiently optimal while local maxima/saddle points are not, despite being impossible to distinguish with only first-order criticality information. To the best of our knowledge, however, no such bounds exist in the general setting, nor do they exist for the vast majority of existing optimization algorithms.

Convergence rate dependence on preconditioner quality One possible quality metric for Φ_t is given by $\eta_t \triangleq \left\|\left(I - \mathcal{H}\left(\theta_t\right) \cdot \Phi_t\right) \cdot \frac{\nabla f(\theta_t)}{\|\nabla f(\theta_t)\|}\right\|_2$. In the convex regime, Nocedal & Wright (2006, Chapter 7.1) assume $\sup_t\left(\eta_t\right) < 1$ and prove that first-order criticality may be reached within

$\mathcal{O}\left(\frac{\log \epsilon}{\log \frac{1+\sup_t(\eta_t)}{2}}\right)$ iterations. Adding an assumption of Lipschitz-continuity of the Hessian, they prove quadratic convergence to first-order criticality. O'Leary-Roseberry et al. (2019), in contrast, do not assume convexity but provide a bound on the parameter gap $\|\theta_t - \theta^*\|_2$ for η_t satisfying the Eisenstat-Walker (Eisenstat & Walker, 1996; Dembo et al., 1982) condition $\eta_t \leq \|\nabla f(\theta_t)\|_2$ on a Tikhonov-regularized Hessian. Like Wang et al. (2016), however, here too the constant in their bound is inversely proportional to $\zeta - \lambda_{\min}(\mathcal{H}(\theta_t))$ with ζ the Tikhonov regularization constant, thus is minimized by taking $\zeta \to \infty$, eliminating all second-order information and reverting to simple gradient descent. As before, this implies looseness due to the empirical success of making use of second-order methods.

C Algorithm ELMO's Descent Rate

An important factor in deciding how much computational effort to invest each optimization iteration is the ratio between the additional computational burden and the corresponding model quality improvement (as measured by the loss function) obtained by that iteration. To that end, we demonstrate that an upper bound on algorithm ELMO's performance has quickly diminishing rewards for additional iterations. Counter-intuitively, this is a good thing - it means that as long as the algorithm converges to an acceptable minimum point, just a few iterations are likely to be necessary in practice - since any more than that will not have much of an effect on the model's quality anyway.

Theorem C.1. *Worst case-optimal descent rate Let f be a function with Lipschitz-continuous Hessian. After t iterations, algorithm ELMO satisfies*

$$f(\theta_0) - f(\theta_t) = \mathcal{O}(\log t) \tag{11}$$

Although the above theorem gives only an upper bound on the model's performance, we demonstrate that it is actually within a constant multiplicative factor of the algorithm's lower bound.

Lemma C.2. *Let $f : \mathbb{R}^n \to \mathbb{R}$ satisfying assumptions 1 and 2. Algorithm ELMO satisfies*

$$\left|m_t^i\left(\Delta\theta_t^{*\top} v_i\right)\right| \leq 5\left|M_t^i\left(\Delta\theta_t^{*\top} v_i\right)\right|$$

D Generalization of previous quasi-Newton preconditioner quality metrics

Notation 10. Taking $(\lambda_i)_{i=1}^n$ the eigenvalues of $\mathcal{H}(\theta)$ for some θ, note that since n is finite, there exist $L^+ \triangleq \max_i\{L^i : \lambda_i > 0\}, L^- \triangleq \max_i\{L^i : \lambda_i \leq 0\}$.

Since most prevalent quasi-Newton algorithms apply a principled approach only to the convex subspaces of the loss function domain space and even then only when the curvature shift is negligible, we examine the special case of our metric when $\lambda_i > 0$ (when the loss function is convex over the domain subspace under examination) and show that our quality metric for quasi-Newton algorithm steps generalizes previous metrics. When $\lambda_i > 0$, we have

$$\left|\Delta\Delta^i\theta_t'\right| = \left|1 - \frac{\nabla f(\theta_t)^\top}{\nabla f(\theta_t)^\top v_i} \cdot (\alpha_t \Phi_t \mathcal{H}(\theta_t)) \cdot v_i \cdot \frac{\sqrt{1 + 2L_t^i \cdot \frac{\left|\nabla f(\theta_t)^\top v_i\right|}{\lambda_i^2}} + 1}{2}\right| \tag{12}$$

Županski (1993) introduce the "Effective Hessian" (a.k.a. the "Preconditioned Hessian") as $\mathcal{I}_t = \alpha_t \Phi_t \mathcal{H}(\theta_t)$, whose condition number used as a quality metric for preconditioners; ideally, $\kappa(\mathcal{I}_t) < \kappa(\mathcal{H}(\theta_t))$. The Effective Hessian may be plainly seen in equation 12.

Mark $r_t \triangleq (I - \mathcal{H}(\theta_t) \cdot \Phi_t) \cdot \frac{\nabla f(\theta_t)}{\nabla f(\theta_t)^\top v_i}$; this is the 1-dimensional version of the quality metric η_t for Φ_t used by Nocedal & Wright (2006, Chapter 7.1) and mentioned in appendix B (now redefined by projecting $\nabla f(\theta_t)$ onto the i-th eigenspace instead of taking its full norm). When $L^+ \approx 0$ (i.e. when the loss function curvature shift is negligible), equation 12 simplifies to

$$\left|\Delta\Delta^i\theta_t'\right| \approx \left|r_t^\top \cdot v_i\right|$$

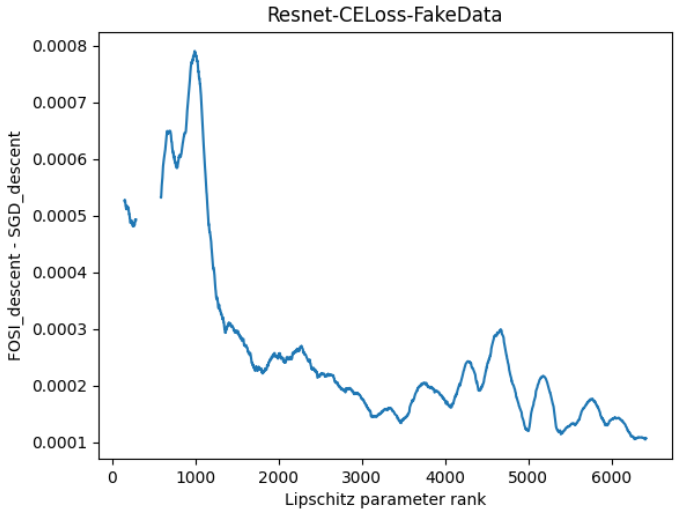

Figure 3: Inverse relation between a convex-subspace Lipschitz parameter and corresponding descent superiority of quasi-Newton method

E A QUALITY PREDICTOR FOR NEWTON'S METHOD

An important challenge is finding the best balance between per-iteration computational burden and expected loss function descent. We set out to provide such a metric due to equation 12 by showing that the expected descent in a given eigenspace is an approximately monotonically decreasing function of the corresponding Lipschitz parameter.

Figure 3 shows an example of this phenomenon by plotting the quasi-Newton superiority (how much better a quasi-Newton method will work than a first-order method, defined as $\left(f\left(\theta_t\right) - f\left(\theta_{t+1}^{Newton}\right)\right) - \left(f\left(\theta_t\right) - f\left(\theta_{t+1}^{SGD}\right)\right)$) against the convex Lipschitz parameter rank. Here too we represent the full spectrum of convex Lipschitz parameters with the single Lipschitz parameter representing the eigenspace with the greatest eigenvalue; nevertheless, a qualitative inverse correlation is clear. Pearson correlation coefficient values (Pearson, 1895) are shown in table 1, as well as p-values of a test of the null hypothesis that the distributions underlying the samples are uncorrelated and normally distributed. The Scipy manual writes:

> The p-value roughly indicates the probability of an uncorrelated system producing datasets that have a Pearson correlation at least as extreme as the one computed from these datasets.

Here too, the detailing of our experiment settings is given in appendix J, as well as further detailing on figure 3.

[(0, 70.16), (0.7, 16.19), (0.8, 17.9), (0.9, 14.65), (0.95, 0.65), (0.99, 0.91), (0.995, 0.65), (0.999, 0.02)]

Dataset	Pearson r	p-value
CIFAR10	-0.245341	10^{-107}
FakeData	-0.026608	0.031120
MNIST	-0.368788	10^{-300}

Table 1: Pearson r inverse correlation between quasi-Newton superiority and Lipschitz parameter

Since the Lipschitz parameters are approximately locally constant throughout training as shown in the previous section, this reverse correlation may be used to help practitioners decide how much computational burden is worth putting into each iteration, given that even an exact Newton step may not be significantly superior to first-order methods when the curvature drift (as measured by Lipschitz parameters) is significantly large; hyperparameter optimization algorithm selection may then follow accordingly. We present experiments validating this selection method in appendix L. Alternatively, practitioners may

choose to use ARC steps instead of first-order methods, when the Lipschitz parameter is significantly large.

F COMPARISON OF ELMO TO SELECT RELATED METHODS

ELMO is strikingly similar to Cauchy's method (not to be confused with Cauchy's Steepest Descent method (Nocedal & Wright, 2006, Chapter 4.1)) and Newton's method mentioned above. In this section, we note the similarity between them, and the sources of the differences between them.

F.1 COMPARISON TO CAUCHY'S METHOD

Cauchy's method (Traub, 1982) is very reminiscent of ELMO:

$$
\begin{aligned}
\left(\theta_{t+1}-\theta_t\right)_{cauchy}^{\top}\cdot v_i &\triangleq -\frac{2}{1+\sqrt{1-2\frac{L_t^i\cdot\nabla f\left(\theta_t\right)^{\top}v_i}{\lambda_i^2\left(\theta_t\right)}}}\cdot\frac{\nabla f\left(\theta_t\right)^{\top}v_i}{\lambda_i\left(\theta_t\right)}\\
&= -\frac{2}{1+\frac{1}{|\lambda_i(\theta_t)|}\cdot\sqrt{\lambda_i^2\left(\theta_t\right)-2L_t^i\cdot\nabla f\left(\theta_t\right)^{\top}v_i}}\frac{\nabla f\left(\theta_t\right)^{\top}v_i}{\lambda_i\left(\theta_t\right)}\\
&= \frac{-2\nabla f\left(\theta_t\right)^{\top}v_i}{\lambda_i\left(\theta_t\right)+\frac{\lambda_i(\theta_t)}{|\lambda_i(\theta_t)|}\cdot\sqrt{\lambda_i^2\left(\theta_t\right)-2L_t^i\cdot\nabla f\left(\theta_t\right)^{\top}v_i}}\\
&= \frac{1}{L_t^i}\cdot\frac{-2L_t^i\cdot\nabla f\left(\theta_t\right)^{\top}v_i}{\lambda_i\left(\theta_t\right)+\frac{\lambda_i(\theta_t)}{|\lambda_i(\theta_t)|}\cdot\sqrt{\lambda_i^2\left(\theta_t\right)-2L_t^i\cdot\nabla f\left(\theta_t\right)^{\top}v_i}}\\
&= \frac{1}{L_t^i}\cdot\frac{\left(\lambda_i^2\left(\theta_t\right)-2L_t^i\cdot\nabla f\left(\theta_t\right)^{\top}v_i\right)-\lambda_i^2\left(\theta_t\right)}{\lambda_i\left(\theta_t\right)+\frac{\lambda_i(\theta_t)}{|\lambda_i(\theta_t)|}\cdot\sqrt{\lambda_i^2\left(\theta_t\right)-2L_t^i\cdot\nabla f\left(\theta_t\right)^{\top}v_i}}\\
&= \frac{\sqrt{\lambda_i^2\left(\theta_t\right)-2L_t^i\cdot\nabla f\left(\theta_t\right)^{\top}v_i}-\sqrt{\lambda_i^2\left(\theta_t\right)}}{L_t^i}\cdot\frac{|\lambda_i\left(\theta_t\right)|}{\lambda_i\left(\theta_t\right)}\\
&= \frac{\sqrt{\lambda_i^2\left(\theta_t\right)-2L_t^i\cdot\nabla f\left(\theta_t\right)^{\top}v_i}-\frac{|\lambda_i(\theta_t)|}{\lambda_i(\theta_t)}\cdot\lambda_i\left(\theta_t\right)}{L_t^i}\cdot\frac{|\lambda_i\left(\theta_t\right)|}{\lambda_i\left(\theta_t\right)}\\
&= \frac{\frac{|\lambda_i(\theta_t)|}{\lambda_i(\theta_t)}\cdot\sqrt{\lambda_i^2\left(\theta_t\right)-2L_t^i\cdot\nabla f\left(\theta_t\right)^{\top}v_i}-\lambda_i\left(\theta_t\right)}{L_t^i}
\end{aligned}
$$

The difference between our minimization step and their step is the sign on the squareroot. The difference stems from removing the absolute value in equation 3's 3rd-order term and taking the negative root of its derivative, due to the difference in goals: we attempt to minimize the function, leading us to select the positive step. They attempt to find the function's critical points, leading them to select the negative step.

F.2 COMPARISON TO NEWTON'S METHOD

Unlike Cauchy's method, Newton's method (in optimization) makes a second-order approximation to the function's gradient. This is equivalent to the Hessian being constant, which is equivalent to

$L_H = 0$. Indeed, taking the limit of equation 7 when $L_H \to 0^+$, we recover Newton's method:

$$\begin{aligned}\lim_{L_H \to 0^+} \Delta\theta_t^{*\top} v_i &= \lim_{L_H \to 0^+} -\frac{2\nabla f(\theta_t)^\top v_i}{\sqrt{\lambda_i^2(\theta_t) - 2L_t^i \cdot \nabla f(\theta_t)^\top v_i} + \lambda_i(\theta_t)} \\ &= \begin{cases} -\frac{\nabla f(\theta_t)^\top v_i}{\lambda_i} & \lambda_i > 0 \\ \infty & \lambda_i < 0 \end{cases}\end{aligned} \tag{13}$$

G Relevance of the Hessian-Lipschitz distribution

One source of interest in the Hessian-Lipschitz distribution is for optimization algorithms (e.g. ARC) that make use of these parameters for the loss function modelling stage of each iteration. This may reduce computational complexity by reducing the number of parameters one must compute at each iteration, however appendix H shows that poorly estimating the Lipschitz parameters can have a detrimental effect on an algorithm's descent rate (thereby increasing the number of iterations the algorithm will require to converge).

Another source of interest in these parameters' distribution is in explaining the effectiveness of second-order quasi-Newton algorithms that implicitly assume the Lipschitz parameters are insignificant (i.e. very close to zero), since their model of the loss function is a quadratic Taylor polynomial (i.e. no curvature shift); this may be seen from equation 12 which shows optimality of Newton's method only when $\lambda_i > 0$ and $L^+ = 0$. As seen in section 5, the Lipschitz parameters are not generally small by any means, however the Lipschitz parameters of the subspaces in which they work (the convex subspaces - see the implementation of Sivan et al. (2024), for instance, which applies Newton's method only on subspaces with significantly convex subspaces) are in fact small in certain settings.

H Convergence rate dependence on Hessian-Lipschitz parameter

As noted by Griewank (1981), the Hessian-Lipschitz parameter (in our case, the respective constants of each eigenspace) may be computationally difficult to obtain precisely, leading some optimization algorithms to estimate it approximately instead of computing it precisely (e.g. ARC). In order to balance the computational burden of computing it to a high degree of exactitude with the degradation of an algorithm's convergence rate that comes with poor estimations, we study the effects of the Hessian-Lipschitz parameter on $M_t^i\left(\Delta\theta_t^\top v_i\right)$.

H.1 Lipschitz Robustness

To address the convergence rate's robustness to overly conservative L_t^i, we consider the case when $L_t^i \to \infty$.

Theorem H.1. *Let $f : \mathbb{R}^n \to \mathbb{R}$ satisfying assumptions 1 and 2. Then*

$$M_t^i\left(\Delta\theta_t^{*\top} v_i\right) = \Theta\left(\frac{1}{\sqrt{L_t^i}}\right)$$

when $L_t^i \to \infty$

Proof.

$$\lim_{L_t^i\to\infty} \frac{M_t^i\left(\Delta\theta_t^{*\top}v_i\right)}{\frac{-12\left(-\nabla f(\theta_t)^\top v_i\right)^{1.5}-36\left(-\nabla f(\theta_t)^\top v_i\right)+\sqrt{2}\sqrt{-\nabla f(\theta_t)^\top v_i}+3\sqrt{2}}{\frac{3}{-\nabla f(\theta_t)^\top v_i}-18\sqrt{2}}\cdot\frac{1}{\sqrt{L_t^i}}}$$

$$= \lim_{L_t^i\to\infty} -\frac{1}{\sqrt{\frac{\lambda_i^2(\theta_t)}{L_t^i\left(-2\cdot\nabla f(\theta_t)^\top v_i\right)}+1}+\frac{\lambda_i(\theta_t)}{\sqrt{L_t^i}\sqrt{-2\cdot\nabla f(\theta_t)^\top v_i}}}$$

$$\cdot\frac{6\sqrt{-\nabla f\left(\theta_t\right)^\top v_i}}{6\sqrt{-\nabla f\left(\theta_t\right)^\top v_i}-2\cdot\nabla f\left(\theta_t\right)^\top v_i}$$

$$-\frac{2\cdot\nabla f\left(\theta_t\right)^\top v_i}{6\sqrt{-\nabla f\left(\theta_t\right)^\top v_i}-2\cdot\nabla f\left(\theta_t\right)^\top v_i}$$

$$\cdot\left(\sqrt{\frac{\lambda_i^2\left(\theta_t\right)}{L_t^i\left(-2\cdot\nabla f\left(\theta_t\right)^\top v_i\right)}+1}-\frac{\lambda_i\left(\theta_t\right)}{\sqrt{L_t^i}\sqrt{-2\cdot\nabla f\left(\theta_t\right)^\top v_i}}\right)^3$$

$$+\frac{1}{\sqrt{L_t^i}}\cdot\frac{1+6\sqrt{2}\nabla f\left(\theta_t\right)^\top v_i}{2\left(6\sqrt{-\nabla f\left(\theta_t\right)^\top v_i}-2\cdot\nabla f\left(\theta_t\right)^\top v_i\right)}\frac{\lambda_i\left(\theta_t\right)\left(\frac{-2\cdot\nabla f(\theta_t)^\top v_i}{\sqrt{\frac{\lambda_i^2(\theta_t)}{L_t^i}-2\cdot\nabla f(\theta_t)^\top v_i}+\frac{\lambda_i(\theta_t)}{\sqrt{L_t^i}}}\right)^2}{\left(\frac{1}{6}+\sqrt{2}\nabla f\left(\theta_t\right)^\top v_i\right)\sqrt{-2\cdot\nabla f\left(\theta_t\right)^\top v_i}}$$

$$= 1$$

□

H.2 Benefit of Lipschitz tightness

To see how minimizing L_t^i as much as possible benefits the bound, we consider the case when $L_t^i \to 0^+$.

Theorem H.2. *Benefit of Lipschitz tightness: concave subspaces*

Let $f : \mathbb{R}^n \to \mathbb{R}$ satisfying assumptions 1 and 2. If $\lambda_i(\theta_t) \le 0$ then

$$M_t^i\left(\Delta\theta_t^{*\top}v_i\right) = \Theta\left(-\frac{1}{L_t^{i,2}}\right)$$

when $L_t^i \to 0^+$

Proof.

$$\lim_{L_t^i\to 0^+}\frac{M_t^i\left(\Delta\theta_t^{*\top}v_i\right)}{\frac{2}{3}\frac{\lambda_i^3(\theta_t)}{L_t^{i,2}}}$$

$$= \lim_{L_t^i\to 0^+}\left(3\left(\frac{\sqrt{1-2L_t^i\cdot\frac{\nabla f(\theta_t)^\top v_i}{(-\lambda_i(\theta_t))^2}}+1}{2}\right)^2-2\left(\frac{\sqrt{1-2L_t^i\cdot\frac{\nabla f(\theta_t)^\top v_i}{(-\lambda_i(\theta_t))^2}}+1}{2}\right)^3\right)$$

$$+L_t^i\cdot\frac{3}{2\lambda_i^3\left(\theta_t\right)}\cdot\left(\sqrt{\lambda_i^2\left(\theta_t\right)-2L_t^i\cdot\nabla f\left(\theta_t\right)^\top v_i}-\lambda_i\left(\theta_t\right)\right)\cdot\nabla f\left(\theta_t\right)^\top v_i$$

$$= 1$$

□

Theorem H.3. *Benefit of Lipschitz tightness: convex subspaces*

Let $f : \mathbb{R}^n \to \mathbb{R}$ satisfying assumptions 1 and 2. If $\lambda_i(\theta_t) > 0$ then

$$M_t^i\left(\Delta\theta_t^{*\top} v_i\right) - M_t^i\left(\lim_{L_t^i \to 0^+} \Delta\theta_t^{*\top} v_i\right) = \Theta\left(L_t^i\right)$$

when $L_t^i \to 0^+$

Proof. We begin by noting that by equation 13, $\lim_{L_t^i \to 0^+} \Delta\theta_t^{*\top} v_i = \frac{\left|\nabla f(\theta_t)^\top v_i\right|}{\lambda_i(\theta_t)}$. Plugging this into M_t^i:

$$\begin{aligned}
&\lim_{L_t^i \to 0^+} \frac{M_t^i\left(\Delta\theta_t^{*\top} v_i\right) - M_t^i\left(\lim_{L_t^i \to 0^+} \Delta\theta_t^{*\top} v_i\right)}{\frac{L_t^i}{\frac{1}{2}\lambda_i(\theta_t)\cdot\frac{\left(\nabla f(\theta_t)^\top v_i\right)^3}{\lambda_i^4(\theta_t)} - \frac{\left(\nabla f(\theta_t)^\top v_i\right)^3}{2\lambda_i^2(\theta_t)}}} \\
&= \lim_{L_t^i \to 0^+} -\frac{\left(\nabla f\left(\theta_t\right)^\top v_i\right)^3}{2\lambda_i^2\left(\theta_t\right)} \cdot \left(\frac{4}{\left(\sqrt{1 - 2L_t^i \cdot \frac{\nabla f(\theta_t)^\top v_i}{\lambda_i(\theta_t)}} + 1\right)^2}\right) \\
&+ \frac{1}{2}\lambda_i\left(\theta_t\right) \cdot \frac{\left(\nabla f\left(\theta_t\right)^\top v_i\right)^3}{\lambda_i^4\left(\theta_t\right)} \cdot \left(\frac{\frac{2\lambda_i(\theta_t)}{\sqrt{\lambda_i^2(\theta_t) - 2L_t^i \cdot \nabla f(\theta_t)^\top v_i} + \lambda_i(\theta_t)}}{2}\right) \\
&\cdot \left(\frac{2\lambda_i^2\left(\theta_t\right)}{\lambda_i\left(\theta_t\right)\sqrt{\lambda_i^2\left(\theta_t\right) - 2L_t^i \cdot \nabla f\left(\theta_t\right)^\top v_i} + \lambda_i^2\left(\theta_t\right)}\right)\left(\frac{2}{1 + \sqrt{1 - 2L_t^i \cdot \frac{\nabla f(\theta_t)^\top v_i}{\lambda_i^2(\theta_t)}}}\right) \\
&- \frac{L_t^i}{4} \cdot \frac{\left(\nabla f\left(\theta_t\right)^\top v_i\right)^4}{\lambda_i^5\left(\theta_t\right)}\left(\frac{2}{\sqrt{1 - 2L_t^i \cdot \frac{\nabla f(\theta_t)^\top v_i}{\lambda_i^2(\theta_t)}} + 1}\right)\left(\frac{2}{\sqrt{1 - 2L_t^i \cdot \frac{\nabla f(\theta_t)^\top v_i}{\lambda_i^2(\theta_t)}} + 1}\right) \\
&\cdot \left(\frac{1 + \frac{2}{\sqrt{1 - 2L_t^i \cdot \frac{\nabla f(\theta_t)^\top v_i}{\lambda_i^2(\theta_t)}} + 1} + \frac{4}{\left(\sqrt{1 - 2L_t^i \cdot \frac{\nabla f(\theta_t)^\top v_i}{\lambda_i^2(\theta_t)}} + 1\right)^2}}{3}\right) \\
&= 1
\end{aligned}$$

□

I Qualitative evidence from previous work on Lipschitz parameters

Experiments by Alain et al. (2018); Sagun et al. (2016); Ghorbani et al. (2019); Gur-Ari et al. (2018) show that the positive eigenvalues of the Hessian remain relatively stable throughout training, while the negative eigenvalues shrink rapidly. Alain et al. (2018) and Sagun et al. (2016) also show that the negative eigenvalues shift chaotically. Gur-Ari et al. (2018) show that when training a network on a classification task with k classes, then at least the eigenspace spanned by the k eigenvectors corresponding to the top k eigenvalues remains very stable. Sivan et al. (2024); Liu et al. (2024) also show that when training a neural network on a variety of tasks, the top k eigenvalues and their corresponding eigenvectors change very slowly. Alain et al. (2018) also show explicitly that the second-order Taylor approximation is a poor approximation of the loss function in the eigenspace corresponding to the negative eigenvalues (the concave eigenspace), but an excellent approximation

in the eigenspace corresponding to the positive eigenvalues (the convex eigenspace); indeed, they show that the optimal step in the convex eigenspace is well estimated by the Newton step, while there is no correlation between the Hessian and the optimal step in the concave eigenspace. Using the Lipschitz parameter as a measure of the rate of change of the Hessian in a given subspace (hence a measure of the quality of a second-order Taylor approximation to a function and its corresponding Newton step), this supports the claim that $L^+ \ll L^-$.

J LIPSCHITZ PARAMETER EXPERIMENTS

We tested our algorithm in 7 scenarios with the PyTorch 1.13.0 framework, each on a single NVIDIA GeForce RTX 3090 GPU with the standard hyperparameters and settings for ARC:

- $\sigma_0^+ = \sigma_0^- = 1$
- $\eta_1 = 0.1, \eta_2 = 0.9$
- $\gamma_1 = \gamma_2 = 2$
- Maximum sub-problem failures = 11
- Maximum sub-problem iterations = 50,
- Sub-problem tolerance = 10^{-6}
- Lanczos eigendecomposition (Garber et al., 2016)
- BFGS trinomial sub-problem solver (Nocedal & Wright, 2006, Chapter 6.1), (Feinman, 2021)
- trinomial sub-problem maximal failures=11
- trinomial sub-problem maximal iterations=50

The test scenarios[4] include combinations of:

- Training ResNet18 artificial neural networks (He et al., 2015) for image classification on MNIST, CIFAR10, and FakeData (random noise in place of images) with Cross-Entropy Loss (CELoss), to evaluate the effect of changing data on the Lipschitz parameters
- Training a CNN for image classification on CIFAR10 with CELoss, to evaluate the effect of changing neural network architecture on the Lipschitz parameters.
- Training a CNN[5] autoencoder[6] (LeCun, 1987) to compress MNIST

The classification CNN architecture:

1. A feature extractor consisting of 2 2D convolutional layers with 6 output channels for the first and 16 output channels for the second. Both had kernel sizes of 5 pixels. Each of these is followed by a ReLU nonlinearity and then 2x2 2D max pooling
2. A 3-layer MLP classification head with hidden sizes (120, 84) and ReLU nonlinearities

The autoencoder CNN architecture:

- Encoder: 4 2D convolutional layers with respective output channel numbers (16,32,32,64) and kernel sizes of 3 pixels for the first two and 5 pixels for the last two. The first two have 1 pixel padding and the last two have 2 pixel paddings. After every layer we apply LeakyReLU nonlinearity and after every 2 layers we apply 2x2 2D max pooling.
- Decoder: 4 composite layers consisting of
  1. a 2D transpose-convolutional layer
  2. LeakyReLU nonlinearity (only for first and third composite layers)

[4] Code available on Github at REDACTED

[5] convolutional neural network

[6] With hidden dimensions 128-64-36-18-9-18-36-64-128, ReLU nonlinearities, and sigmoid nonlinearity on the output

3. a 2d convolutional layer
4. LeakyReLU nonlinearity

- Decoder hidden channel sizes: 32-32-16-16-16-16-3
- Decoder kernel sizes: 2-5-5-5-2-3-5-3
- All strides are of size 1, except for the first and third transpose-convolutional layers of the decoder, with stride of size 2
- Decoder paddings: 0-2-2-2-0-1-2-1

Each experiment took several hours to run. All experiments (including those from above) shown in figure 4.

One caveat is that due to computational constraints, we use stochastic minibatch training for the neural networks instead of using the full batch to compute the gradient and Hessian-vector products at each iteration (see Bertsekas (1996) for an introduction to minibatch Monte-Carlo estimation of a sum). However, Cartis et al. (2011a), notes that the adaptive Lipschitz parameter estimates may account for this variance by being greater than the actual Lipschitz parameters. Thus, our claims of $L^+ \ll 1$ are not affected (since our experiments effectively provide an upper bound on L^+) while our claims of $L^- \gg 0$ are weakened. Since there is no reason to expect the variance on L^- to be significantly greater than the variance on L^+, however, our experiments remain valid.

For visual clarity, the quasi-Newton superiority measurements in 3 are presented after:

1. Clipping extreme values to the 10% - 90% quantile range
2. Gaussian smoothing, consisting of a rolling window of size 300 and standard deviation of 100

J.1 Computation of Lipschitz parameters

We modified the standard ARC algorithm to compute distinct Lipschitz parameters for the eigenspaces corresponding to the minimal and maximal eigenvalues. Pseudocode for this algorithm is given below.

While lines 3-18 of `EigenARC` may technically be usable as the `LIPSCHITZ` subroutine of algorithm `ELMO` above, each iteration requires $\Omega(n)$ evaluations of the loss function, which will be computationally expensive if $n \gg 0$ and if the loss function is computationally heavy. This may be ameliorated by performing these calculations only for a small subset of the eigenspaces like Sivan et al. (2024), however we leave this to future work.

K AMOS experiment details

In section 4 we present tests demonstrating the application of `AMOS` to training NanoGP on the TinyShakespeare dataset. Below are the hyperparameters we selected for the experiment.

- Our AdamW reference run takes the tuned hyperparameters from vanilla NanoGPT, namely - learning rate = $6 \cdot 10^{-4}$, weight decay = 10^{-1}, $\beta_1 = 0.9$, $\beta_2 = 0.95$.
- Our first-order optimizer is SGD with learning rate set to $1.25 \cdot 10^{-}5$, selected by grid hyperparameter search. We also tried adding a Cosine Annealing scheduler for SGD, but this harmed SGD's performance and had no qualitative effect on the training trajectory comparison graph, so it is not included in our results.
- Our second-order optimizer is Sophia, with $\rho = 0.01$ and otherwise Karpathy (2022)'s standard AdamW hyperparameters.
- Our Sophia and SGD reference optimization trajectories use optimizers with the same hyperparameters but without dynamic optimizer selection (instead using pure SGD all the way through or pure Sophia).
- The momentum coefficient for our meta-optimizer $\alpha_L = 0.99$, and the Lipschitz threshold $L_{thresh} = 2 \cdot 10^{-10}$, $\epsilon_2 = 10^{-12}$.

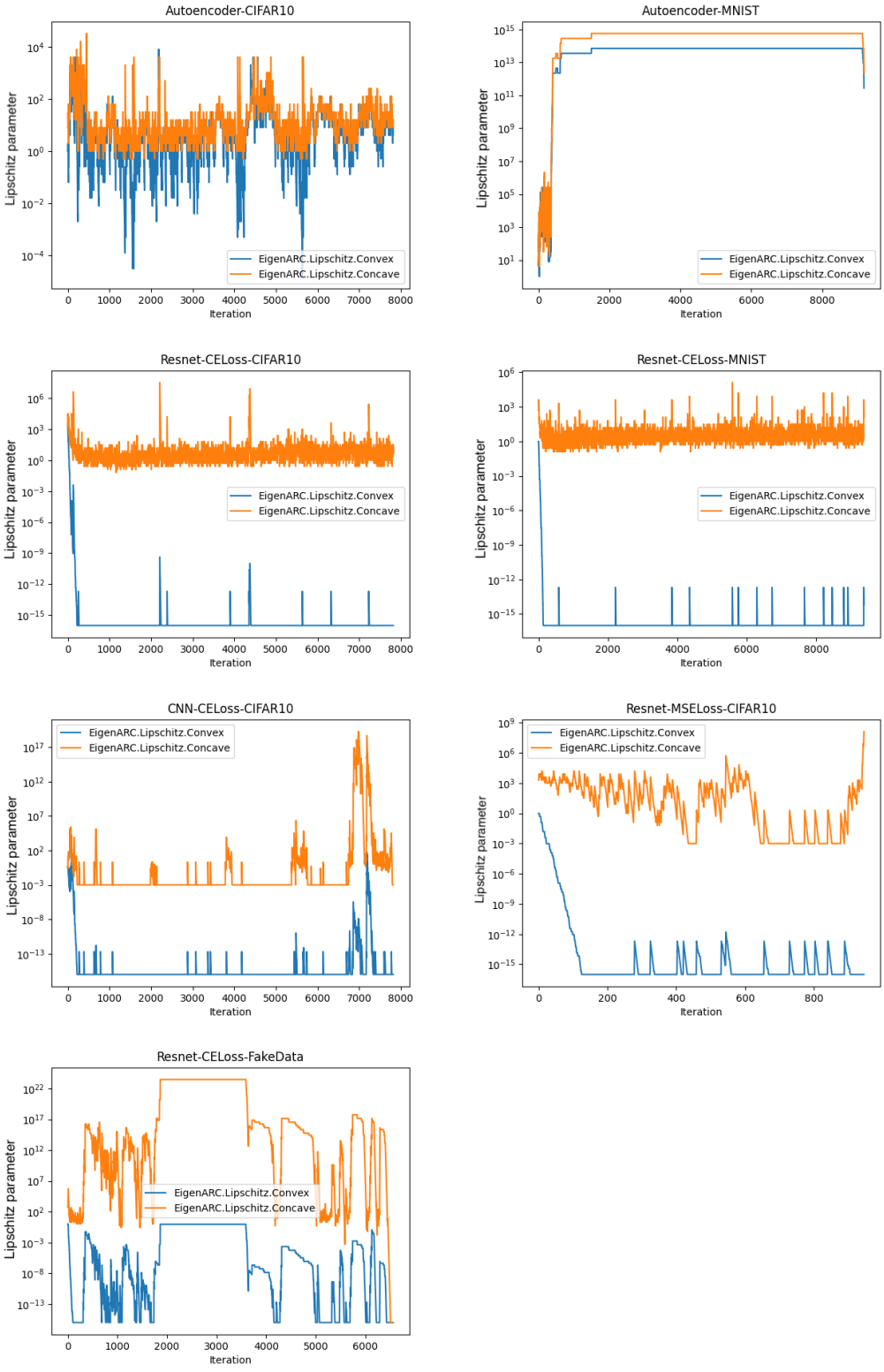

Figure 4: Comparisons of convex-subspace Lipschitz parameters to concave-subspace Lipschitz parameters. *Logarithmic scale*

Algorithm 3 Algorithm `EigenARC`

Require: $\epsilon \in \mathbb{R}^+, \theta_0 \in \mathbb{R}^n, \gamma_1 > 1 > \gamma_2 > 0, \eta_2 \geq \eta_1 > 0, \left(L_0^i\right)_{i=1}^n > 0$, `EIGEN`, `BASE_OPT`

$t \leftarrow 0$
while $\|\nabla f(\theta_t)\|_2 > \epsilon$ **do** ▷ While `BASE_OPT` hasn't converged yet
  $(\lambda_i, v_i)_{i=1}^n \leftarrow$ `EIGEN` $(\mathcal{H}(\theta_{\mathtt{t}}))$
  if `ASSESS_LIPSCHITZ` $\left((\mathtt{L}_{\mathtt{t}}^{\mathtt{i}})_{\mathtt{i=1}}^{\mathtt{n}}\right) > \eta_2$ **then** ▷ Overly conservative L_t^i
    $\left(L_t^i\right)_{i=1}^n \leftarrow \gamma_2 \cdot \left(L_t^i\right)_{i=1}^n$
  else
    if `ASSESS_LIPSCHITZ` $\left((\mathtt{L}_{\mathtt{t}}^{\mathtt{i}})_{\mathtt{i=1}}^{\mathtt{n}}\right) < \eta_1$ **then** ▷ Overly liberal L_t^i
      while `ASSESS_LIPSCHITZ` $\left((\mathtt{L}_{\mathtt{t}}^{\mathtt{i}})_{\mathtt{i=1}}^{\mathtt{n}}\right) > \eta_1$ **do** ▷ Raise all L_t^i assessment is passed
        $\left(L_t^i\right)_{i=1}^n \leftarrow \gamma_1 \cdot \left(L_t^i\right)_{i=1}^n$
      end while
      for i=1,...,n **do** ▷ Reduce the L_t^i that can be reduced without violating assessment
        while `ASSESS_LIPSCHITZ` $\left((\mathtt{L}_{\mathtt{t}}^{\mathtt{i}})_{\mathtt{i=1}}^{\mathtt{n}}\right) > \eta_1$ **do**
          $L_t^i \leftarrow \frac{L_t^i}{\gamma_1}$
        end while
        $L_t^i \leftarrow \gamma_1 \cdot L_t^i$
      end for
    end if
  end if
  $\theta_{t+1} \leftarrow$ `BASE_OPT` $(\theta_{\mathtt{t}})$
  $t \leftarrow t + 1$
end while
return $\left(L_{\hat{t}}^i\right)_{i=1,\hat{t}=1}^{n,t}$

procedure ASSESS_LIPSCHITZ($\left(\hat{L_t^i}\right)_{i=1}^n$)
  return $\frac{f(\theta_t) - f\left(\theta_t + \sum_{i=1}^n \Delta{\theta_t^*}^\top v_i \left(\hat{L_t^i}\right) \cdot v_i\right)}{-\sum_{i=1}^n M_t^i \left(\Delta{\theta_t^*}^\top v_i \left(\hat{L_t^i}\right)\right)}$
end procedure

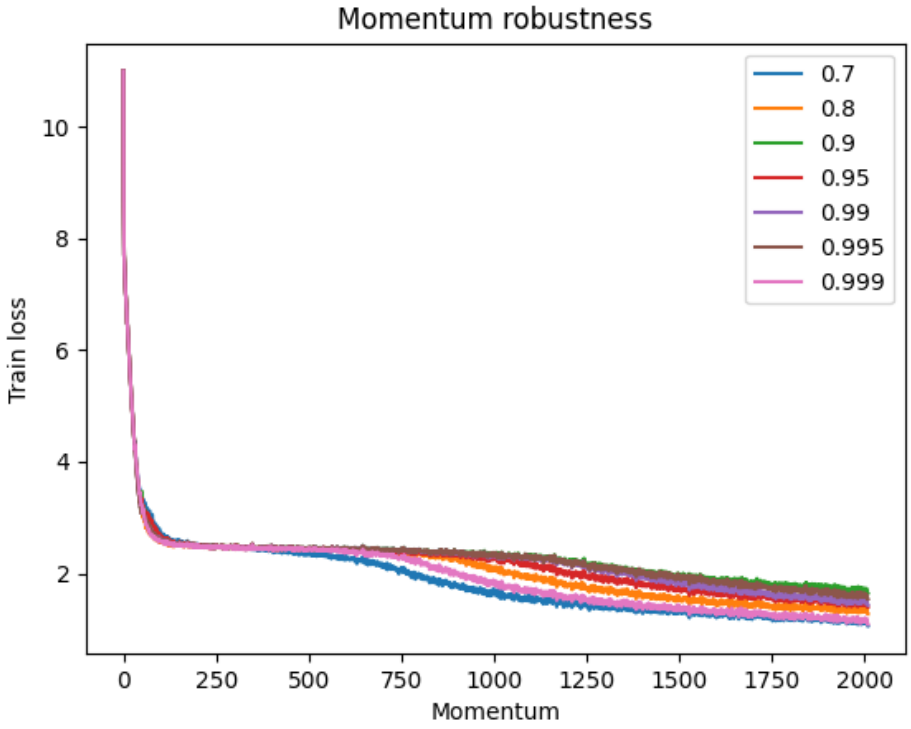

Figure 5: Training trajectories of AMOS with various different momentum settings. There is little variation in the long run.

Lipschitz momentum (α_L)	Offloaded parameters (%)
0.7	16.19
0.8	17.90
0.9	14.65
0.95	0.65
0.99	0.91
0.995	0.65
0.999	0.02

Table 2: Percent of parameters offloaded to SGD

- For hardware efficiency reasons, we transfer parameters to SGD at a per-tensor granularity instead of per-scalar (although we suggest subdividing tensors into constant sizes in future work). The mean Lipschitz parameter of the entire tensor is compared against the preset threshold to determine if it is transferred to the first-order optimizer or not.

To demonstrate our AMOS's robustness to hyperparameter selection, we rerun the above test with threshold L_{thresh} selected by equation 8 (thus requiring no tuning). Training trajectories for various Lipschitz-estimation momentums α_L shown in figure 5; we see that the momentum has little effect on the training trajectory. In particular, we compare the training- and test-loss of the experiment with $\alpha_L = 0.7$ against the aforementioned standard AdamW baseline in figure 6; it is evident that there is little difference between the training trajectories.

In each of the above runs, we report the percent of parameters offloaded to SGD in table 2.

Caveat: our Lipschitz initialization scheme (initialization to 0) biases the Lipschitz parameters towards 0, with greater bias maintained with greater momentum (hence the reverse correlation of parameter offload with Lipschitz-momentum). We leave initialization schemes to future work.

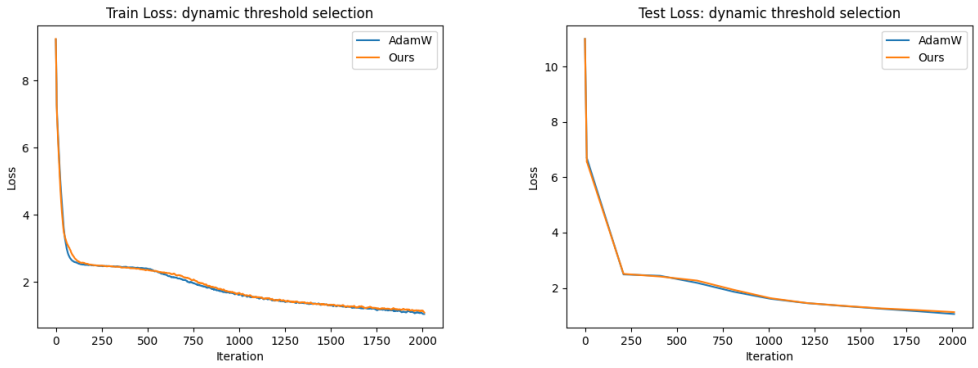

Figure 6: Comparison of AMOS-combined SGD and Sophia vs. AdamW. We see little difference between the two despite offloading 16% of parameters to cheaper SGD optimizer.

The settings for this experiment are identical to those above, with the following exceptions:

- SGD's learning rate reduced to $3.125 \cdot 10^{-6}$
- $\epsilon_2 = 10^{-15}$
- Each tensor's Lipschitz parameter is chosen with maximum aggregation across the tensor instead of mean aggregation

L LIPSCHITZ-AIDED OPTIMIZER SELECTION

In this section, we demonstrate the use of convex Lipschitz parameters to select the best optimizer for our use case. Due to the relative constancy of Lipschitz parameters throughout the training process (after an initial warmup phase) in different settings, we can select optimizers for each setting based on the following rule: **quasi-Newton optimizers hold an advantage over first-order optimizers when the convex Lipschitz parameters are small**. As discussed in section 5, the convex Lipschitz parameters in the image autoencoder training setting are far larger than those in the image classification setting, so we compare a quasi-Newton optimizer against first-order methods in these settings to validate our rule.

FOSI Sivan et al. (2024) is a variant of Saddle-Free Newton Dauphin et al. (2014) which applies Newton iterations in the domain space subspaces spanned by the dominant eigenvectors of the Hessian, and a first-order "base optimizer" in the remaining subspaces. We use FOSI as our representative second-order optimizer due to its computational effectiveness, capability to adjust the computational complexity of each iteration by adjusting the number of "dominant" eigenvectors to compute (fewer eigenvectors comes at the cost of a poorer Hessian approximation by approximating the Hessian with a lower-rank matrix, although this is somewhat mitigated by applying the base optimizer in these subspaces), and fairness of comparison (since its integration of first-order optimizers allows us to compare the effect of second-order optimization in the dominant eigenspaces against first-order optimization in these spaces, while all else is held equal - the remaining subspaces are both treated by the same first-order optimizers).

Experiment results may be seen in figure 7.

The experiments are run with the same settings as before, with FOSI augmenting SGD and Adam respectively and Savitzky-Golay order-2 filtering with a window size of 5000 for clarity of visualization. It may be clearly seen that FOSI second-order augmentation is beneficial only in the classification setting, due to the small convex Lipschitz parameters.

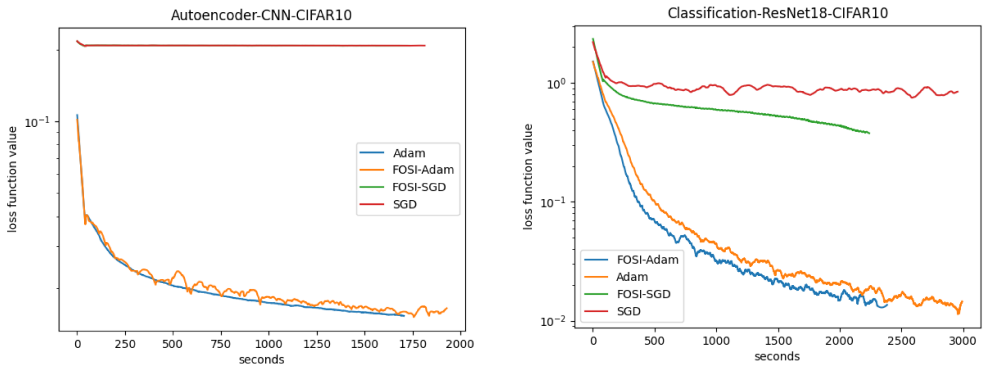

(a) The setting in which we train a CNN on an autoencoder task has large convex Lipschitz parameters throughout training

(b) The setting in which we train ResNet18 on a classification task has small convex Lipschitz parameters throughout training

Figure 7: Comparison of second-order optimizers against first-order optimizers in settings with different sized convex Lipschitz parameters. Second-order optimizers only hold an advantage over first-order optimizers (thus justifying their additional computational complexity) when the convex Lipschitz parameters are small.

M PROOFS

M.1 PRELIMINARY LEMMAS

Before we can get started, we prove a few basic lemmas.

Lemma M.1.

$$\forall_{x\geq -1}: \sqrt{1+x} \leq 1+\frac{x}{2}$$

Proof. Mark $g: \mathbb{R} \to \mathbb{R}, g(x) = 1+\frac{x}{2}-\sqrt{1+x}$. We have

$g'(x) = \frac{1}{2}\left(1-\frac{1}{\sqrt{1+x}}\right)$

$g''(x) = \frac{1}{4}\left(\frac{1}{(1+x)^{\frac{3}{2}}}\right)$

g is convex due to its second derivative being positive for all $x > -1$. Therefore, its sole critical point $x = 0$ obtained from the derivative is a minimum, and $\forall_{x\geq -1}: g(x) \geq g(0) = 0$ □

Corollary M.1.1.

$$\forall_{x\in\mathbb{R}^+}\forall_{y\geq -x}: \sqrt{x+y} \leq \sqrt{x}+\frac{y}{2\sqrt{x}}$$

Proof.

$$\sqrt{x+y} = \sqrt{x}\sqrt{1+\frac{y}{x}} \leq \sqrt{x}\left(1+\frac{y}{2x}\right) = \sqrt{x}+\frac{y}{2\sqrt{x}}$$

□

Lemma. *Let $f: \mathbb{R}^n \to \mathbb{R}$ satisfy assumptions 1 and 2. Then*

$$m_t^i\left(\Delta\theta_t^{*\top} v_i\right) \leq M_t^i\left(\Delta\theta_t^{*\top} v_i\right) \leq 0 \tag{14}$$

Proof. The first inequality stems from the trivial fact that $m_t^i \leq M_t^i$.

The second inequality follows from the fact that (by design), $\Delta\theta_t^{*\top} v_i$ is a minimizer of $M_t^i\left(\Delta\theta_t^{\top} v_i\right)$, but

$$M_t^i(0) = 0$$

□

Lemma. *3.2 Minmax preconditioner*

$$\underset{\Phi_t \in \mathbb{R}^{n\times n}}{\arg\min} \left|\Delta\Delta^i\theta_t\left(\Phi_t\right)\right| = \left(\frac{\mathcal{H}\left(\theta_t\right) + \sqrt{\left(\mathcal{H}\left(\theta_t\right)\right)^2 + 2V \cdot diag\left(L_t^i \cdot \left|\nabla f\left(\theta_t\right)^\top v_i\right|\right)_{i=1}^n \cdot V^\top}}{2}\right)^{-1}$$

Proof.

$$\begin{aligned}\left|\Delta\Delta^i\theta_t\right| &= \left|\nabla f\left(\theta_t\right)^\top \left(\Phi_t - \frac{2}{\lambda_i + \sqrt{\lambda_i^2 - 2L_t^i \cdot \nabla f\left(\theta_t\right)^\top v_i}} I\right) v_i\right| \\ &= \left|\nabla f\left(\theta_t\right)^\top \left(\Phi_t - \left(\frac{\mathcal{H}\left(\theta_t\right) + \sqrt{\left(\mathcal{H}\left(\theta_t\right)\right)^2 + 2L_t^i \cdot \left|\nabla f\left(\theta_t\right)^\top v_i\right| I}}{2}\right)^{-1}\right) v_i\right|\end{aligned}$$

and the result follows from developing the second parenthesized term for all n dimensions of the domain space. □

M.2 Lemma 3.1: Eigenspace Descent

Working with assumptions 1 and equation 2, Dennis & Schnabel (1983, Lemma 4.1.14) prove the following:

Lemma M.2.

$$f\left(\theta_{t+1}\right) - f\left(\theta_t\right) \leq \nabla f\left(\theta_t\right)^T \cdot \Delta\theta_t + \frac{1}{2}\Delta\theta_t^T \mathcal{H}\left(\theta_t\right)\Delta\theta_t + \frac{1}{6}L_H\left\|\Delta\theta_t\right\|_2^3 \tag{15}$$

Much like algorithm ELMO, minimizing equation 15 would maximize [a bound on] the descent given by iteration t. However, previous works such as Nesterov & Polyak (2006) note the difficulty of minimizing this 3rd-order n-dimensional polynomial, even when L_H is known. Indeed, Cartis et al. (2011a) propose minimizing it iteratively over a growing subspace, with each iteration's minimization subspace a superset of the previous iterations' (in practice, they use the Hessian's Krylov subspaces, initialized with the gradient). In our theoretical analysis however, we have the freedom to simply take the most natural decomposition of the space into subspaces, the eigenspaces of the Hessian. This does not limit the practicality of our approach, however, since Lanczos methods allow one to obtain elements of this decomposition. In fact, Sivan et al. (2024) demonstrate experimentally that decomposing the parameter space into multiple eigenspaces and optimizing each separately can significantly speed up optimization wall time, despite the additional computational burden of the Lanczos iterations, because of the regularizing effect this has on the function in each of the subspaces (by reducing the variance of the Hessian eigenvalues). Ghorbani et al. (2019) also show the benefits of reducing this variance.

Lemma. *3.1 Eigenspace Descent Bounds*

Let $f : \mathbb{R}^n \to \mathbb{R}$ be a function satisfying assumptions 1 and 2, and let $\theta_{t+1} \in \mathbb{R}^n$. Marking $\Delta\theta_t = \theta_{t+1} - \theta_t$, we have

$$\exists_{\left(L_t^i\right)_{i=1}^n \in \left(\mathbb{R}^+\right)^n} : f\left(\theta_{t+1}\right) - f\left(\theta_t\right) \leq \sum_{i=1}^n M_t^i\left(\Delta\theta_t^\top v_i\right) \tag{16}$$

$$\exists_{\left(L_t^i\right)_{i=1}^n \in \left(\mathbb{R}^+\right)^n} : f\left(\theta_{t+1}\right) - f\left(\theta_t\right) \geq \sum_{i=1}^n m_t^i\left(\Delta\theta_t^\top v_i\right) \tag{17}$$

We give 2 proofs of the above lemma. The first proof is far simpler and relies on the standard spectral norm-Lipschitz continuous Hessian assumption given by equation 2 instead of assumption 2:

Proof. Beginning with Nesterov & Polyak (2006, Lemma 1) for the first inequality,

$$\begin{aligned}
\left|f\left(\theta_{t+1}\right)-f\left(\theta_t\right)-\left(\nabla f\left(\theta_t\right)^{\top}\left(\theta_{t+1}-\theta_t\right)+\left(\theta_{t+1}-\theta_t\right)^{\top}\mathcal{H}\left(\theta_t\right)\left(\theta_{t+1}-\theta_t\right)\right)\right| \\
\leq L_H\left\|\theta_{t+1}-\theta_t\right\|_2^3 \\
\left|f\left(\theta_{t+1}\right)-f\left(\theta_t\right)-\left(\sum_{i=1}^{n}\left(\nabla f\left(\theta_t\right)^{\top}v_i\cdot\left(\theta_{t+1}-\theta_t\right)^{\top}v_i+\lambda_i\left(\left(\theta_{t+1}-\theta_t\right)^{\top}v_i\right)^2\right)\right)\right| \\
\leq L_H\left\|\sum_{i=1}^{n}\left(\theta_{t+1}-\theta_t\right)^{\top}v_i v_i^{\top}\right\|_2^3 \\
\leq L_H\left(\sum_{i=1}^{n}\left\|\left(\theta_{t+1}-\theta_t\right)^{\top}v_i v_i^{\top}\right\|_2\right)^3 \\
= L_H\cdot n^3\left(\sum_{i=1}^{n}\frac{1}{n}\left|\left(\theta_{t+1}-\theta_t\right)^{\top}v_i\right|\right)^3 \\
\leq L_H\cdot n^3\left(\frac{1}{n}\sum_{i=1}^{n}\left|\left(\theta_{t+1}-\theta_t\right)^{\top}v_i\right|^3\right) \\
= L_H\cdot n^2\sum_{i=1}^{n}\left|\left(\theta_{t+1}-\theta_t\right)^{\top}v_i\right|^3 \\
= \sum_{i=1}^{n}\tilde{L_H}\cdot\left|\left(\theta_{t+1}-\theta_t\right)^{\top}v_i\right|^3
\end{aligned}$$

with

1. the second inequality being a representation of $\theta_{t+1}-\theta_t$ over the (orthogonal) Hessian eigenbasis
2. the third inequality due to the triangle inequality
3. the fourth inequality due to Jensen's inequality

□

Our first proof of lemma 3.1 is simple, but leaves something to be desired due to its lack of per-eigenspace Lipschitz parameters and due to the presence of n^2 in the bound, which can be very large, as noted in section A. The first proof's assumption of equation 2 is also easily seen to be no weaker than assumption 2 (meaning that assuming equation 2 implies assumption 2) by taking $L_R \triangleq L_t^i \triangleq L_H$ for all $t \in [T], i \in [n]$. To address these concerns, we make use of assumption 2, and give a second (though more complicated) proof for lemma 3.1. We'll prove only the upper bound, as a proof for the lower bound is similar.

Proof.

$$
\begin{aligned}
&f(\theta_{t+1}) - f(\theta_t) \\
&= \int_0^1 \nabla f(\theta_t + y(\theta_{t+1} - \theta_t))^\top (\theta_{t+1} - \theta_t)\, dy \\
&= \nabla f(\theta_t)^\top (\theta_{t+1} - \theta_t) + \int_0^1 (\nabla f(\theta_t + y(\theta_{t+1} - \theta_t)) - \nabla f(\theta_t))^\top (\theta_{t+1} - \theta_t)\, dy \\
&= \nabla f(\theta_t)^\top (\theta_{t+1} - \theta_t) + \int_0^1 \left(\int_0^1 y \mathcal{H}(\theta_t + yz(\theta_{t+1} - \theta_t))(\theta_{t+1} - \theta_t)\, dz \right)^\top (\theta_{t+1} - \theta_t)\, dy \\
&= \nabla f(\theta_t)^\top (\theta_{t+1} - \theta_t) + \int_0^1 \int_0^1 y(\theta_{t+1} - \theta_t)^\top \mathcal{H}(\theta_t + yz(\theta_{t+1} - \theta_t))(\theta_{t+1} - \theta_t)\, dydz \\
&= \nabla f(\theta_t)^\top (\theta_{t+1} - \theta_t) + (\theta_{t+1} - \theta_t)^\top \mathcal{H}(\theta_t)(\theta_{t+1} - \theta_t) \\
&+ \underbrace{\int_0^1 \int_0^1 y(\theta_{t+1} - \theta_t)^\top (\mathcal{H}(\theta_t + yz(\theta_{t+1} - \theta_t)) - \mathcal{H}(\theta_t))(\theta_{t+1} - \theta_t)\, dydz}_{Z}
\end{aligned}
$$

with the first and third equalities due to the fundamental theorem of calculus.

Mark the Hessian eigendecompositions as follows:

$$
\begin{aligned}
\mathcal{H}(\theta_t + yz(\theta_{t+1} - \theta_t)) &= \tilde{V}\tilde{\Lambda}\tilde{V}^\top \\
\mathcal{H}(\theta_t) &= V\Lambda V^\top
\end{aligned}
$$

with diagonal $\Lambda = diag\left(\lambda_i\right)_{i=1}^n, \tilde{\Lambda} = diag\left(\tilde{\lambda_i}\right)_{i=1}^n$ and orthogonal (due to the Hermitian nature of Hessian matrices) matrices $V, \tilde{V}$.

$$
\begin{aligned}
Z &= \int_0^1 \int_0^1 y(\theta_{t+1} - \theta_t)^\top \left(\tilde{V}\tilde{\Lambda}\tilde{V}^\top - V\Lambda V^\top\right)(\theta_{t+1} - \theta_t)\, dydz \\
&= \int_0^1 \int_0^1 y(\theta_{t+1} - \theta_t)^\top \left(V\tilde{\Lambda}V^\top - V\Lambda V^\top\right)(\theta_{t+1} - \theta_t)\, dydz \\
&+ \int_0^1 \int_0^1 y(\theta_{t+1} - \theta_t)^\top \left(\tilde{V}\tilde{\Lambda}\tilde{V}^\top - V\tilde{\Lambda}V^\top\right)(\theta_{t+1} - \theta_t)\, dydz
\end{aligned}
$$

Focusing on the first term,

$$
\begin{aligned}
&= \int_0^1 \int_0^1 y(\theta_{t+1} - \theta_t)^\top V\left(\tilde{\Lambda} - \Lambda\right)V^\top(\theta_{t+1} - \theta_t)\, dydz \\
&= \int_0^1 \int_0^1 y \sum_{j=1}^n \sum_{i=1}^n (\theta_{t+1} - \theta_t)^\top v_i \cdot (\theta_{t+1} - \theta_t)^\top v_j \cdot v_j^\top V\left(\tilde{\Lambda} - \Lambda\right)V^\top v_i dydz \\
&= \int_0^1 \int_0^1 y \cdot \sum_{i=1}^n \left((\theta_{t+1} - \theta_t)^\top v_i\right)^2 \cdot \left(\tilde{\lambda_i} - \lambda_i\right) dydz \\
&\leq \sum_{i=1}^n L_t^i \cdot \left|(\theta_{t+1} - \theta_t)^\top v_i\right|^3 \cdot \int_0^1 \int_0^1 y \cdot yz \cdot dydz \\
&= \sum_{i=1}^n \frac{L_t^i}{6} \cdot \left|(\theta_{t+1} - \theta_t)^\top v_i\right|^3
\end{aligned}
$$

As for the second term,

$$\begin{aligned}
&\int_0^1\int_0^1 y\left(\theta_{t+1}-\theta_t\right)^\top\left(\tilde{V}\tilde{\Lambda}\tilde{V}^\top-V\tilde{\Lambda}V^\top\right)\left(\theta_{t+1}-\theta_t\right)dydz\\
&=\int_0^1\int_0^1 y\left(\theta_{t+1}-\theta_t\right)^\top\left(\tilde{V}-V\right)\tilde{\Lambda}\left(\tilde{V}+V\right)^\top\left(\theta_{t+1}-\theta_t\right)dydz\\
&+\int_0^1\int_0^1 y\left(\theta_{t+1}-\theta_t\right)^\top\left(\left(\tilde{V}\tilde{\Lambda}V^\top\right)^\top-\tilde{V}\tilde{\Lambda}V^\top\right)\left(\theta_{t+1}-\theta_t\right)dydz\\
&=\int_0^1\int_0^1 y\left(\theta_{t+1}-\theta_t\right)^\top\left(\tilde{V}-V\right)\tilde{\Lambda}\left(\tilde{V}+V\right)^\top\left(\theta_{t+1}-\theta_t\right)dydz\\
&\le\int_0^1\int_0^1 y\cdot\left\|\tilde{V}-V\right\|_2\cdot\left\|\tilde{\Lambda}\right\|_2\cdot\left\|\tilde{V}+V\right\|_2\cdot\left\|\theta_{t+1}-\theta_t\right\|_2^2\cdot dydz\\
&\le\frac{1}{3}\cdot L_R\left\|\tilde{\Lambda}\right\|_2\cdot\left\|\theta_{t+1}-\theta_t\right\|_2^3\\
&=\frac{1}{3}\cdot L_R\left\|\tilde{\Lambda}\right\|_2\cdot\left\|\left(\theta_{t+1}-\theta_t\right)V^\top\right\|_2^3\\
&\le\frac{\sqrt{n}}{3}\cdot L_R\left\|\tilde{\Lambda}\right\|_2\cdot\left\|\left(\theta_{t+1}-\theta_t\right)V^\top\right\|_3^3\\
&=\frac{\sqrt{n}}{3}\cdot L_R\left\|\tilde{\Lambda}\right\|_2\cdot\sum_{i=1}^n\left|\left(\theta_{t+1}-\theta_t\right)V^\top\cdot e_i\right|^3\\
&=\sum_{i=1}^n\frac{\sqrt{n}}{3}\cdot L_R\left\|\tilde{\Lambda}\right\|_2\cdot\left|\left(\theta_{t+1}-\theta_t\right)v_i\right|^3
\end{aligned}$$

with

- the first 4 transfers similar to those in the proof of lemma M.4
- the third equality due to orthonormality
- the third inequality due to the L_p norms inequality
- e_i indicating the 1-hot vector with a 1 in the i-th entry

Putting it all together (and representing $\theta_{t+1}-\theta_t$ by its coordinate vector over the eigenbasis of $\mathcal{H}\left(\theta_t\right)$):

$$\begin{aligned}
f\left(\theta_{t+1}\right)-f\left(\theta_t\right)\le\sum_{i=1}^n\nabla f\left(\theta_t\right)^\top v_i\cdot\left(\theta_{t+1}-\theta_t\right)^\top v_i+\lambda_i\left(\theta_t\right)\cdot\left(\left(\theta_{t+1}-\theta_t\right)^\top v_i\right)^2\\
+\left(\frac{L_t^i}{6}+\frac{\sqrt{n}}{3}\cdot L_R\cdot L_H\right)\cdot\left|\left(\theta_{t+1}-\theta_t\right)v_i\right|^3
\end{aligned}$$

□

To understand the relationship between our assumption 2 and the more standard equation 2, we further prove that the combination of assumption 2 and a bounded spectrum assumption will be no weaker than equation 2:

Lemma M.3. *Let $A\in\mathbb{R}^{n\times n}, v\in\mathbb{R}^n$. Then $v^\top\left(A^\top-A\right)v=0$.*

Proof.

$$v^\top\left(A^\top-A\right)v=\left(v^\top\left(A^\top-A\right)v\right)^\top=v^\top\left(A-A^\top\right)v=-v^\top\left(A^\top-A\right)v$$

□

Theorem M.4. *Let $f : \mathbb{R}^n \to \mathbb{R}$ be a function satisfying assumptions 1 and 2, and assume $\exists_{\lambda_{\sup} \in \mathbb{R}} \forall_{\theta \in \mathbb{R}^n} \forall_{i \in [n]} : \lambda_i(\theta) \leq \lambda_{\sup}$. Then equation 2 is satisfied.*

Proof.

$$\begin{aligned}
\left|p^\top \left(\mathcal{H}(\theta) - \mathcal{H}(\varphi)\right) p\right| &= \left|p^\top \left(V\Lambda V^\top - \tilde{V}\tilde{\Lambda}\tilde{V}^\top\right) p\right| \\
&\leq \left|p^\top \left(V\Lambda V^\top - \tilde{V}\Lambda\tilde{V}^\top\right) p\right| + \left|p^\top \tilde{V}\left(\Lambda - \tilde{\Lambda}\right)\tilde{V}^\top p\right| \\
&= \left|p^\top \left(V - \tilde{V}\right)\Lambda\left(V + \tilde{V}\right)^\top p\right| + \left|p^\top \tilde{V}\left(\Lambda - \tilde{\Lambda}\right)\tilde{V}^\top p\right| \\
&\leq \left\|V - \tilde{V}\right\|_2 \cdot \|\Lambda\|_2 \cdot \left\|V + \tilde{V}\right\|_2 \cdot \|p\|_2^2 + \left\|\tilde{V}^\top p\right\|_2^2 \cdot \left\|\Lambda - \tilde{\Lambda}\right\|_2 \\
&\leq \left(2L_R \cdot \sup_{\theta' \in \mathbb{R}^n, i \in \mathbb{R}} \lambda_i(\theta')\right) \cdot \|\theta - \varphi\|_2 + \max_i L^i \cdot \|\theta - \varphi\|_2 \\
&\leq \left(2L_H \cdot \lambda_{\sup} + L_H\right) \cdot \|\theta - \varphi\|_2
\end{aligned}$$

with

- the first inequality due to the triangle inequality
- the second equality due to lemma M.3
- the second inequality due to the Cauchy-Schwartz inequality
- the third inequality due to the triangle inequality, and the fact that all of an orthonormal matrix's eigenvalues equal one of $\{-1, 1\}$

□

M.3 Theorem C.1: Worst case-optimal descent rate

Before we can prove theorem C.1, we need to upper bound equation 7.

Lemma M.5. *Minmax stepsize bound*

If $\lambda_i \geq 0$ then

$$\Delta\theta_t^{*\top} v_i = \mathcal{O}\left(\sqrt{\left|\nabla f(\theta_t)^\top v_i\right|}\right)$$

If $\lambda_i < 0$ then

$$\Delta\theta_t^{*\top} v_i = \mathcal{O}\left(|\lambda_i|\right)$$

Proof. For i s.t. $0 \leq \lambda_i \leq \sqrt{L_t^i \cdot \left|\nabla f\left(\theta_t\right)^\top v_i\right|}$ we use corollary M.1.1 with $x = 2L_t^i \cdot \left|\nabla f\left(\theta_t\right)^\top v_i\right|$ to obtain

$$\begin{aligned}
\Delta\theta_t^{*\top} v_i &= \frac{\sqrt{\lambda_i^2 + 2L_t^i \cdot \left|\nabla f\left(\theta_t\right)^\top v_i\right|} - \lambda_i}{L_t^i} \\
&\leq \sqrt{2} \cdot \sqrt{\frac{\left|\nabla f\left(\theta_t\right)^\top v_i\right|}{L_t^i}} + \frac{\frac{\lambda_i^2}{2} \cdot \frac{1}{\sqrt{2L_t^i \cdot \left|\nabla f(\theta_t)^\top v_i\right|}} - \lambda_i}{L_t^i} \\
&\leq \sqrt{2} \cdot \sqrt{\frac{\left|\nabla f\left(\theta_t\right)^\top v_i\right|}{L_t^i}} + \frac{1}{2\sqrt{2}} \cdot \sqrt{\frac{\left|\nabla f\left(\theta_t\right)^\top v_i\right|}{L_t^i}} \\
&= \frac{5}{2\sqrt{2}} \cdot \sqrt{\frac{\left|\nabla f\left(\theta_t\right)^\top v_i\right|}{L_t^i}}
\end{aligned}$$

For i s.t. $\lambda_i > \sqrt{L_t^i \cdot \left|\nabla f\left(\theta_t\right)^\top v_i\right|}$ we use corollary M.1.1 with $x = \lambda_i^2$ to obtain

$$\Delta\theta_t^{*\top} v_i \leq \frac{\left|\nabla f\left(\theta_t\right)^\top v_i\right|}{\lambda_i} \leq \frac{\left|\nabla f\left(\theta_t\right)^\top v_i\right|}{\sqrt{L_t^i \cdot \left|\nabla f\left(\theta_t\right)^\top v_i\right|}} = \sqrt{\frac{\left|\nabla f\left(\theta_t\right)^\top v_i\right|}{L_t^i}}$$

For i s.t. $\lambda_i < 0$, we again use corollary M.1.1 with $x = \lambda_i^2$ to obtain

$$\Delta\theta_t^{*\top} v_i = \frac{2L_t^i \cdot \left|\nabla f\left(\theta_t\right)^\top v_i\right|}{L_t^i\left(\sqrt{\lambda_i^2 + 2L_t^i \cdot \left|\nabla f\left(\theta_t\right)^\top v_i\right|} - |\lambda_i|\right)} \leq \frac{2\left|\lambda_i\right|}{L_t^i} = \mathcal{O}\left(|\lambda_i|\right)$$

□

We are now ready to prove theorem C.1.

Theorem. *Worst case-optimal descent rate Let f be a function with Lipschitz-continuous Hessian. After t iterations, algorithm* `ELMO` *satisfies*

$$f\left(\theta_0\right) - f\left(\theta_t\right) = \mathcal{O}\left(\log t\right) \tag{18}$$

Proof. Cartis et al. (2012a) give $\left|\nabla f\left(\theta_t\right)^\top v_i\right| = \mathcal{O}\left(\frac{1}{t^{\frac{2}{3}}}\right)$ and $\forall_{i:\lambda_i<0} : |\lambda_i| = \mathcal{O}\left(\frac{1}{\sqrt[3]{t}}\right)$ for the ARC optimization algorithm, of which algorithm `ELMO` is a special case (the case where ARC perfectly estimates the Hessian Lipschitz parameter).

Making use of lemma M.5 and noting that $m_t^i\left(\Delta\theta_t^{*\top} v_i\right) \leq 0$ by equation 14:

$$\left|m_t^i\left(\Delta\theta_t^{*\top} v_i\right)\right| = \left|\nabla f\left(\theta_t\right)^\top v_i\right| \cdot \Delta\theta_t^{*\top} v_i + \frac{-\lambda_i}{2} \cdot \left(\Delta\theta_t^{*\top} v_i\right)^2 + \frac{L_t^i}{6} \cdot \left(\Delta\theta_t^{*\top} v_i\right)^3$$

For i s.t. $\lambda_i \geq 0$:

$$\begin{aligned}
&\leq \left|\nabla f\left(\theta_t\right)^\top v_i\right| \cdot \mathcal{O}\left(\sqrt{\frac{\left|\nabla f\left(\theta_t\right)^\top v_i\right|}{L_t^i}}\right) + \mathcal{O}\left(\sqrt{\frac{\left|\nabla f\left(\theta_t\right)^\top v_i\right|}{L_t^i}}\right)^3 \\
&= \mathcal{O}\left(\left|\nabla f\left(\theta_t\right)^\top v_i\right|^{1.5}\right) = \mathcal{O}\left(\left(\frac{1}{t^{\frac{2}{3}}}\right)^{1.5}\right) = \mathcal{O}\left(\frac{1}{t}\right)
\end{aligned}$$

For i s.t. $\lambda_i < 0$:

$$\leq \left|\nabla f\left(\theta_t\right)^\top v_i\right| \cdot \mathcal{O}\left(|\lambda_i|\right) + |\lambda_i| \cdot \left(\mathcal{O}\left(|\lambda_i|\right)\right)^2 + \mathcal{O}\left(|\lambda_i|\right)^3 = \mathcal{O}\left(\left|\nabla f\left(\theta_t\right)^\top v_i\right| \cdot |\lambda_i| + |\lambda_i|^3\right)$$
$$= \mathcal{O}\left(\frac{1}{t^{\frac{2}{3}}} \cdot \frac{1}{\sqrt[3]{t}} + \frac{1}{t}\right) = \mathcal{O}\left(\frac{1}{t}\right)$$

Finally, we have

$$\begin{aligned} f\left(\theta_0\right) - f\left(\theta_T\right) &= \sum_{t=0}^{T-1} f\left(\theta_t\right) - f\left(\theta_{t+1}\right) \\ &\leq \sum_{t=0}^{T-1} \left|m_t^i\left(\Delta\theta_t^{*\top} v_i\right)\right| \\ &\leq \sum_{t=1}^{T-1} \mathcal{O}\left(\frac{1}{t}\right) \\ &\leq \mathcal{O}\left(\log t + \gamma + \frac{1}{2t}\right) \\ &= \mathcal{O}\left(\log t\right) \end{aligned}$$

with $\gamma \approx 0.57721$ as the Euler-Mascheroni constant and Young (1991) for the last inequality. □

M.4 THEOREM C.2

Theorem.

$$\left|m_t^i\left(\Delta\theta_t^{*\top} v_i\right)\right| \leq 5\left|M_t^i\left(\Delta\theta_t^{*\top} v_i\right)\right|$$

Proof. Due to equation 14, we have $\frac{m_t^i\left(\Delta\theta_t^{*\top} v_i\right)}{M_t^i\left(\Delta\theta_t^{*\top} v_i\right)} = \left|\frac{m_t^i\left(\Delta\theta_t^{*\top} v_i\right)}{M_t^i\left(\Delta\theta_t^{*\top} v_i\right)}\right|$. Now:

$$\begin{aligned} &\frac{m_t^i\left(\Delta\theta_t^{*\top} v_i\right)}{M_t^i\left(\Delta\theta_t^{*\top} v_i\right)} \\ &= \frac{\nabla f\left(\theta_t\right)^\top v_i \cdot \Delta\theta_t^{*\top} v_i + \frac{\lambda_i}{2}\left(\Delta\theta_t^{*\top} v_i\right)^2 - \frac{L_t^i}{6} \cdot \left|\Delta\theta_t^{*\top} v_i\right|^3}{\nabla f\left(\theta_t\right)^\top v_i \cdot \Delta\theta_t^{*\top} v_i + \frac{\lambda_i}{2}\left(\Delta\theta_t^{*\top} v_i\right)^2 + \frac{L_t^i}{6} \cdot \left|\Delta\theta_t^{*\top} v_i\right|^3} \\ &= \frac{-\left|\nabla f\left(\theta_t\right)^\top v_i\right| + \frac{\lambda_i}{2}\frac{\sqrt{\lambda_i^2 + 2L_t^i\left|\nabla f(\theta_t)^\top v_i\right|} - \lambda_i}{L_t^i} - \frac{L_t^i}{6} \cdot \left(\frac{\sqrt{\lambda_i^2 + 2L_t^i\left|\nabla f(\theta_t)^\top v_i\right|} - \lambda_i}{L_t^i}\right)^2}{-\left|\nabla f\left(\theta_t\right)^\top v_i\right| + \frac{\lambda_i}{2}\frac{\sqrt{\lambda_i^2 + 2L_t^i\left|\nabla f(\theta_t)^\top v_i\right|} - \lambda_i}{L_t^i} + \frac{L_t^i}{6} \cdot \left(\frac{\sqrt{\lambda_i^2 + 2L_t^i\left|\nabla f(\theta_t)^\top v_i\right|} - \lambda_i}{L_t^i}\right)^2} \\ &= \frac{5\left(\lambda_i\sqrt{\lambda_i^2 + 2L_t^i\left|\nabla f\left(\theta_t\right)^\top v_i\right|} - \lambda_i^2\right) - 8L_t^i\left|\nabla f\left(\theta_t\right)^\top v_i\right|}{\left(\lambda_i\sqrt{\lambda_i^2 + 2L_t^i\left|\nabla f\left(\theta_t\right)^\top v_i\right|} - \lambda_i^2\right) - 4L_t^i\left|\nabla f\left(\theta_t\right)^\top v_i\right|} \end{aligned}$$

If $\lambda_i = 0$, then

$$\frac{m_t^i\left(\Delta\theta_t^{*\top} v_i\right)}{M_t^i\left(\Delta\theta_t^{*\top} v_i\right)} = 2$$

If $\lambda_i > 0$, then

$$\frac{m_t^i\left(\Delta\theta_t^{*\top}v_i\right)}{M_t^i\left(\Delta\theta_t^{*\top}v_i\right)} = \frac{5\frac{\sqrt{1+2\frac{L_t^i|\nabla f(\theta_t)^\top v_i|}{\lambda_i^2}}-1}{\frac{L_t^i|\nabla f(\theta_t)^\top v_i|}{\lambda_i^2}} - 8}{\frac{\sqrt{1+2\frac{L_t^i|\nabla f(\theta_t)^\top v_i|}{\lambda_i^2}}-1}{\frac{L_t^i|\nabla f(\theta_t)^\top v_i|}{\lambda_i^2}} - 4} \leq \lim_{x\to\infty} \frac{5\frac{\sqrt{1+2x}-1}{x} - 8}{\frac{\sqrt{1+2x}-1}{x} - 4} = 2$$

due to the monotonic increasing nature of $\psi_5 : \mathbb{R}^+ \to \mathbb{R}, \psi_5(x) = \frac{5\frac{\sqrt{1+2x}-1}{x}-8}{\frac{\sqrt{1+2x}-1}{x}-4}$.

If $\lambda_i < 0$, then

$$\frac{m_t^i\left(\Delta\theta_t^{*\top}v_i\right)}{M_t^i\left(\Delta\theta_t^{*\top}v_i\right)} = \frac{5\frac{\sqrt{1+2\frac{L_t^i|\nabla f(\theta_t)^\top v_i|}{|\lambda_i|^2}}+1}{\frac{L_t^i|\nabla f(\theta_t)^\top v_i|}{|\lambda_i|^2}} + 8}{\frac{\sqrt{1+2\frac{L_t^i|\nabla f(\theta_t)^\top v_i|}{|\lambda_i|^2}}+1}{\frac{L_t^i|\nabla f(\theta_t)^\top v_i|}{|\lambda_i|^2}} + 4} \leq \lim_{x\to 0^+} \frac{5\frac{\sqrt{1+2x}+1}{x} + 8}{\frac{\sqrt{1+2x}+1}{x} + 4} = 5$$

due to the monotonic decreasing nature of $\psi_6 : \mathbb{R}^+ \to \mathbb{R}, \psi_6(x) = \frac{5\frac{\sqrt{1+2x}+1}{x}+8}{\frac{\sqrt{1+2x}+1}{x}+4}$. □

M.5 Theorem 3.3: Worst-case descent rate for arbitrary optimizers

Theorem. *Relative Descent Rate*

- $$\left|\frac{M_t^i\left(\Delta\theta_t^{\top}v_i\right) - M_t^i\left(\Delta\theta_t^{*\top}v_i\right)}{M_t^i\left(\Delta\theta_t^{*\top}v_i\right)}\right| = \Theta\left(\left|\Delta\Delta^i\theta_t'\right|^2\right)$$

- $$\left|\frac{m_t^i\left(\Delta\theta_t^{\top}v_i\right) - m_t^i\left(\Delta\theta_t^{*\top}v_i\right)}{m_t^i\left(\Delta\theta_t^{*\top}v_i\right)}\right| = \Theta\left(\left|\Delta\Delta^i\theta_t'\right|\right) \tag{19}$$

Proof. For the first part of the lemma,

$$
\begin{aligned}
&\left|\frac{M_t^i\left(\Delta\theta_t^\top v_i\right)-M_t^i\left(\Delta\theta_t^{*\top} v_i\right)}{M_t^i\left(\Delta\theta_t^{*\top} v_i\right)}\right| \\
&=\frac{\nabla f\left(\theta_t\right)^\top \cdot v_i \cdot\left(\left(\theta_{t+1}-\theta_t\right)^\top v_i-\Delta\theta_t^{*\top} v_i\right)}{\Delta\theta_t^{*\top} v_i \cdot \nabla f\left(\theta_t\right)^\top v_i+\frac{1}{2}\lambda_i\left(\Delta\theta_t^{*\top} v_i\right)^2+\frac{L_t^i}{6}\left(\Delta\theta_t^{*\top} v_i\right)^3} \\
&+\frac{\frac{1}{2}\lambda_i \cdot\left(\left(\left(\theta_{t+1}-\theta_t\right)^\top v_i\right)^2-\left(\Delta\theta_t^{*\top} v_i\right)^2\right)}{\Delta\theta_t^{*\top} v_i \cdot \nabla f\left(\theta_t\right)^\top v_i+\frac{1}{2}\lambda_i\left(\Delta\theta_t^{*\top} v_i\right)^2+\frac{L_t^i}{6}\left(\Delta\theta_t^{*\top} v_i\right)^3} \\
&+\frac{\frac{L_t^i}{6} \cdot\left(\left(\left(\theta_{t+1}-\theta_t\right)^\top \cdot v_i\right)^3-\left(\Delta\theta_t^{*\top} v_i\right)^3\right)}{\Delta\theta_t^{*\top} v_i \cdot \nabla f\left(\theta_t\right)^\top v_i+\frac{1}{2}\lambda_i\left(\Delta\theta_t^{*\top} v_i\right)^2+\frac{L_t^i}{6}\left(\Delta\theta_t^{*\top} v_i\right)^3} \\
&=\Delta\Delta^i\theta_t'\left(\frac{\frac{L_t^i}{6} \cdot\left(\Delta\Delta^i\theta_t'^2+2\Delta\Delta^i\theta_t'+3\right) \cdot\left(\Delta\theta_t^{*\top} v_i\right)^2}{\frac{L_t^i}{6}\left(\Delta\theta_t^{*\top} v_i\right)^2+\frac{1}{2}\lambda_i\Delta\theta_t^{*\top} v_i-\left|\nabla f\left(\theta_t\right)^\top v_i\right|}\right. \\
&+\frac{\lambda_i \cdot\left(\frac{1}{2}\Delta\Delta^i\theta_t'+1\right) \cdot \Delta\theta_t^{*\top} v_i}{\frac{L_t^i}{6}\left(\Delta\theta_t^{*\top} v_i\right)^2+\frac{1}{2}\lambda_i\Delta\theta_t^{*\top} v_i-\left|\nabla f\left(\theta_t\right)^\top v_i\right|} \\
&\left.-\frac{\left|\nabla f\left(\theta_t\right)^\top \cdot v_i\right|}{\frac{L_t^i}{6}\left(\Delta\theta_t^{*\top} v_i\right)^2+\frac{1}{2}\lambda_i\Delta\theta_t^{*\top} v_i-\left|\nabla f\left(\theta_t\right)^\top v_i\right|}\right) \\
&=\Delta\Delta^i\theta_t'\left(\frac{\frac{1}{6} \cdot\left(\Delta\Delta^i\theta_t'^2+2\Delta\Delta^i\theta_t'+3\right) \cdot \frac{\left(\sqrt{\lambda_i^2+2L_t^i \cdot\left|\nabla f\left(\theta_t\right)^\top v_i\right|}-\lambda_i\right)^2}{L_t^i}}{\frac{1}{6}\frac{\left(\sqrt{\lambda_i^2+2L_t^i \cdot\left|\nabla f\left(\theta_t\right)^\top v_i\right|}-\lambda_i\right)^2}{L_t^i}+\frac{1}{2}\lambda_i\frac{\sqrt{\lambda_i^2+2L_t^i \cdot\left|\nabla f\left(\theta_t\right)^\top v_i\right|}-\lambda_i}{L_t^i}-\left|\nabla f\left(\theta_t\right)^\top v_i\right|}\right. \\
&+\frac{\lambda_i \cdot\left(\frac{1}{2}\Delta\Delta^i\theta_t'+1\right) \cdot\left(\frac{\sqrt{\lambda_i^2+2L_t^i \cdot\left|\nabla f\left(\theta_t\right)^\top v_i\right|}-\lambda_i}{L_t^i}\right)}{\frac{1}{6}\frac{\left(\sqrt{\lambda_i^2+2L_t^i \cdot\left|\nabla f\left(\theta_t\right)^\top v_i\right|}-\lambda_i\right)^2}{L_t^i}+\frac{1}{2}\lambda_i\frac{\sqrt{\lambda_i^2+2L_t^i \cdot\left|\nabla f\left(\theta_t\right)^\top v_i\right|}-\lambda_i}{L_t^i}-\left|\nabla f\left(\theta_t\right)^\top v_i\right|} \\
&\left.-\frac{\left|\nabla f\left(\theta_t\right)^\top \cdot v_i\right|}{\frac{1}{6}\frac{\left(\sqrt{\lambda_i^2+2L_t^i \cdot\left|\nabla f\left(\theta_t\right)^\top v_i\right|}-\lambda_i\right)^2}{L_t^i}+\frac{1}{2}\lambda_i\frac{\sqrt{\lambda_i^2+2L_t^i \cdot\left|\nabla f\left(\theta_t\right)^\top v_i\right|}-\lambda_i}{L_t^i}-\left|\nabla f\left(\theta_t\right)^\top v_i\right|}\right) \\
&=\Delta\Delta^i\theta_t' \cdot\left(\frac{\Delta\Delta^i\theta_t'+2\Delta\Delta^i\theta_t'^2}{\lambda_i\sqrt{\lambda_i^2+2L_t^i \cdot\left|\nabla f\left(\theta_t\right)^\top v_i\right|}-\lambda_i^2-4L_t^i\left|\nabla f\left(\theta_t\right)^\top v_i\right|} \cdot \lambda_i^2\right. \\
&+\frac{2\left(\Delta\Delta^i\theta_t'^2+2\Delta\Delta^i\theta_t'\right)}{\lambda_i\sqrt{\lambda_i^2+2L_t^i \cdot\left|\nabla f\left(\theta_t\right)^\top v_i\right|}-\lambda_i^2-4L_t^i\left|\nabla f\left(\theta_t\right)^\top v_i\right|} \cdot L_t^i \cdot\left|\nabla f\left(\theta_t\right)^\top v_i\right| \\
&\left.-\frac{\Delta\Delta^i\theta_t'+2\Delta\Delta^i\theta_t'^2}{\lambda_i\sqrt{\lambda_i^2+2L_t^i \cdot\left|\nabla f\left(\theta_t\right)^\top v_i\right|}-\lambda_i^2-4L_t^i\left|\nabla f\left(\theta_t\right)^\top v_i\right|} \cdot \lambda_i\sqrt{\lambda_i^2+2L_t^i \cdot\left|\nabla f\left(\theta_t\right)^\top v_i\right|}\right)
\end{aligned}
$$

If $\lambda_i = 0$:

$$= -\Delta\Delta^i {\theta'_t}^2 \cdot \left(1 + \frac{1}{2}\Delta\Delta^i \theta'^2_t\right)$$

If $\lambda_i > 0$:

$$\begin{aligned}
&= \Delta\Delta^i \theta'^2_t \cdot \frac{1}{\frac{1}{\sqrt{1+2\frac{L_t^i \cdot \left|\nabla f(\theta_t)^\top v_i\right|}{\lambda_i^2}}+1} - 2} \\
&\cdot \left(\left(\Delta\Delta^i \theta'_t + 2\right) - \left(1 + 2\Delta\Delta^i \theta'_t\right) \cdot \frac{1}{1 + \sqrt{1 + 2\frac{L_t^i \cdot \left|\nabla f(\theta_t)^\top v_i\right|}{\lambda_i^2}}} \right) \\
&= \Delta\Delta^i \theta'^2_t \cdot \left(\Delta\Delta^i \theta'_t - 1 - \sqrt{1 + 2\frac{L_t^i \cdot \left|\nabla f\left(\theta_t\right)^\top v_i\right|}{\lambda_i^2}} \cdot \left(\Delta\Delta^i \theta'_t + 2\right) \right) \\
&\cdot \frac{1}{1 + 2\sqrt{1 + 2\frac{L_t^i \cdot \left|\nabla f(\theta_t)^\top v_i\right|}{\lambda_i^2}}} \\
&= \Delta\Delta^i {\theta'_t}^3 \cdot \frac{1}{1 + 2\sqrt{1 + 2\frac{L_t^i \cdot \left|\nabla f(\theta_t)^\top v_i\right|}{\lambda_i^2}}} \\
&- \Delta\Delta^i \theta'^2_t \cdot \left(1 + \frac{1}{2} \left(1 - \frac{1}{1 + 2\sqrt{1 + 2\frac{L_t^i \cdot \left|\nabla f(\theta_t)^\top v_i\right|}{\lambda_i^2}}} \right) \cdot \Delta\Delta^i \theta'_t \right) \\
&= \left(\frac{3}{2} \frac{1}{1 + 2\sqrt{1 + 2\frac{L_t^i \cdot \left|\nabla f(\theta_t)^\top v_i\right|}{\lambda_i^2}}} - \frac{1}{2} \right) \cdot \Delta\Delta^i {\theta'_t}^3 - \Delta\Delta^i \theta'^2_t
\end{aligned}$$

Proving that

$$\frac{1}{1 + 2\sqrt{1 + 2\frac{L_t^i \cdot \left|\nabla f(\theta_t)^\top v_i\right|}{\lambda_i^2}}} \in \left(0, \frac{1}{3}\right]$$

would conclude the proof for this case. This is easily proven, by noting that

$$\psi_1 : \mathbb{R}^+ \to \mathbb{R}, \psi_1\left(x\right) = \left(1 + 2\sqrt{1 + 2x}\right)^{-1}$$

is monotonic and satisfies

$$\lim_{x \to 0^+} \psi_1\left(x\right) = \frac{1}{3}$$

$$\lim_{x \to \infty} \psi_1\left(x\right) = 0$$

If, on the other hand, $\lambda_i < 0$:

$$= -\Delta\Delta^i\theta_t'^2 \cdot \left(\left(1 + 2\Delta\Delta^i\theta_t'\right) - \frac{3}{2}\Delta\Delta^i\theta_t' \cdot \frac{\frac{L_t^i \left|\nabla f(\theta_t)^\top v_i\right|}{|\lambda_i|^2}}{\frac{L_t^i \left|\nabla f(\theta_t)^\top v_i\right|}{|\lambda_i|^2} + \frac{1}{4}\sqrt{1 + 2\frac{L_t^i \cdot \left|\nabla f(\theta_t)^\top v_i\right|}{|\lambda_i|^2}} + \frac{1}{4}} \right)$$

$$= \left(\frac{3}{2} \cdot \frac{\frac{L_t^i \left|\nabla f(\theta_t)^\top v_i\right|}{|\lambda_i|^2}}{\frac{L_t^i \left|\nabla f(\theta_t)^\top v_i\right|}{|\lambda_i|^2} + \frac{1}{4}\sqrt{1 + 2\frac{L_t^i \cdot \left|\nabla f(\theta_t)^\top v_i\right|}{|\lambda_i|^2}} + \frac{1}{4}} - 2 \right) \Delta\Delta^i\theta_t'^3 - \Delta\Delta^i\theta_t'^2$$

Proving that

$$\frac{\frac{L_t^i \left|\nabla f(\theta_t)^\top v_i\right|}{|\lambda_i|^2}}{\frac{L_t^i \left|\nabla f(\theta_t)^\top v_i\right|}{|\lambda_i|^2} + \frac{1}{4}\sqrt{1 + 2\frac{L_t^i \cdot \left|\nabla f(\theta_t)^\top v_i\right|}{|\lambda_i|^2}} + \frac{1}{4}} \in [0, 1)$$

would conclude the proof for this case as well. This is easily proven, by noting that

$$\psi_2 : \mathbb{R}^+ \to \mathbb{R}, \psi_2(x) = \frac{x}{x + \frac{1}{4}\sqrt{1 + 2x} + \frac{1}{4}}$$

is monotonic and satisfies

$$\lim_{x \to 0^+} \psi_2(x) = 0$$

$$\lim_{x \to \infty} \psi_2(x) = 1$$

For the second part of the lemma,

$$
\begin{aligned}
&\left|\frac{m_t^i\left(\Delta\theta_t^\top v_i\right)-m_t^i\left(\Delta\theta_t^{*\top} v_i\right)}{m_t^i\left(\Delta\theta_t^{*\top} v_i\right)}\right| \\
&=\frac{\nabla f\left(\theta_t\right)^\top \cdot v_i \cdot\left(\left(\theta_{t+1}-\theta_t\right)^\top v_i-\Delta\theta_t^{*\top} v_i\right)}{\Delta\theta_t^{*\top} v_i \cdot \nabla f\left(\theta_t\right)^\top v_i+\frac{1}{2}\lambda_i\left(\Delta\theta_t^{*\top} v_i\right)^2-\frac{L_t^i}{6}\left(\Delta\theta_t^{*\top} v_i\right)^3} \\
&+\frac{\frac{1}{2}\lambda_i \cdot\left(\left(\left(\theta_{t+1}-\theta_t\right)^\top v_i\right)^2-\left(\Delta\theta_t^{*\top} v_i\right)^2\right)}{\Delta\theta_t^{*\top} v_i \cdot \nabla f\left(\theta_t\right)^\top v_i+\frac{1}{2}\lambda_i\left(\Delta\theta_t^{*\top} v_i\right)^2-\frac{L_t^i}{6}\left(\Delta\theta_t^{*\top} v_i\right)^3} \\
&-\frac{\frac{L_t^i}{6} \cdot\left(\left(\left(\theta_{t+1}-\theta_t\right)^\top \cdot v_i\right)^3-\left(\Delta\theta_t^{*\top} v_i\right)^3\right)}{\Delta\theta_t^{*\top} v_i \cdot \nabla f\left(\theta_t\right)^\top v_i+\frac{1}{2}\lambda_i\left(\Delta\theta_t^{*\top} v_i\right)^2-\frac{L_t^i}{6}\left(\Delta\theta_t^{*\top} v_i\right)^3} \\
&=\Delta\Delta^i\theta_t'\left(\frac{\frac{-L_t^i}{6} \cdot\left(\Delta\Delta^i\theta_t'^2+2\Delta\Delta^i\theta_t'+3\right)}{-\frac{L_t^i}{6}\left(\Delta\theta_t^{*\top} v_i\right)^2+\frac{1}{2}\lambda_i\Delta\theta_t^{*\top} v_i-\left|\nabla f\left(\theta_t\right)^\top v_i\right|} \cdot\left(\Delta\theta_t^{*\top} v_i\right)^2\right. \\
&+\frac{\lambda_i \cdot\left(\frac{1}{2}\Delta\Delta^i\theta_t'+1\right)}{-\frac{L_t^i}{6}\left(\Delta\theta_t^{*\top} v_i\right)^2+\frac{1}{2}\lambda_i\Delta\theta_t^{*\top} v_i-\left|\nabla f\left(\theta_t\right)^\top v_i\right|} \cdot \Delta\theta_t^{*\top} v_i \\
&\left.-\frac{\left|\nabla f\left(\theta_t\right)^\top \cdot v_i\right|}{-\frac{L_t^i}{6}\left(\Delta\theta_t^{*\top} v_i\right)^2+\frac{1}{2}\lambda_i\Delta\theta_t^{*\top} v_i-\left|\nabla f\left(\theta_t\right)^\top v_i\right|}\right) \\
&=\Delta\Delta^i\theta_t'\left(\frac{-\frac{1}{6} \cdot\left(\Delta\Delta^i\theta_t'^2+2\Delta\Delta^i\theta_t'+3\right) \cdot \frac{\left(\sqrt{\lambda_i^2+2L_t^i \cdot\left|\nabla f\left(\theta_t\right)^\top v_i\right|}-\lambda_i\right)^2}{L_t^i}}{-\frac{1}{6}\frac{\left(\sqrt{\lambda_i^2+2L_t^i \cdot\left|\nabla f\left(\theta_t\right)^\top v_i\right|}-\lambda_i\right)^2}{L_t^i}+\frac{1}{2}\lambda_i\frac{\sqrt{\lambda_i^2+2L_t^i \cdot\left|\nabla f\left(\theta_t\right)^\top v_i\right|}-\lambda_i}{L_t^i}-\left|\nabla f\left(\theta_t\right)^\top v_i\right|}\right. \\
&+\frac{\lambda_i \cdot\left(\frac{1}{2}\Delta\Delta^i\theta_t'+1\right) \cdot\left(\frac{\sqrt{\lambda_i^2+2L_t^i \cdot\left|\nabla f\left(\theta_t\right)^\top v_i\right|}-\lambda_i}{L_t^i}\right)}{-\frac{1}{6}\frac{\left(\sqrt{\lambda_i^2+2L_t^i \cdot\left|\nabla f\left(\theta_t\right)^\top v_i\right|}-\lambda_i\right)^2}{L_t^i}+\frac{1}{2}\lambda_i\frac{\sqrt{\lambda_i^2+2L_t^i \cdot\left|\nabla f\left(\theta_t\right)^\top v_i\right|}-\lambda_i}{L_t^i}-\left|\nabla f\left(\theta_t\right)^\top v_i\right|} \\
&\left.-\frac{\left|\nabla f\left(\theta_t\right)^\top \cdot v_i\right|}{-\frac{1}{6}\frac{\left(\sqrt{\lambda_i^2+2L_t^i \cdot\left|\nabla f\left(\theta_t\right)^\top v_i\right|}-\lambda_i\right)^2}{L_t^i}+\frac{1}{2}\lambda_i\frac{\sqrt{\lambda_i^2+2L_t^i \cdot\left|\nabla f\left(\theta_t\right)^\top v_i\right|}-\lambda_i}{L_t^i}-\left|\nabla f\left(\theta_t\right)^\top v_i\right|}\right)
\end{aligned}
$$

$$
\begin{aligned}
&= \Delta\Delta^i\theta'_t \left(\frac{12\lambda_i \cdot \sqrt{\lambda_i^2 + 2L_t^i \cdot \left|\nabla f\left(\theta_t\right)^\top v_i\right|} - 12\lambda_i^2 - 12L_t^i \left|\nabla f\left(\theta_t\right)^\top \cdot v_i\right|}{5\lambda_i \sqrt{\lambda_i^2 + 2L_t^i \cdot \left|\nabla f\left(\theta_t\right)^\top v_i\right|} - 5\lambda_i^2 - 8L_t^i \cdot \left|\nabla f\left(\theta_t\right)^\top v_i\right|} \right. \\
&+ \frac{7\lambda_i \cdot \left(\sqrt{\lambda_i^2 + 2L_t^i \cdot \left|\nabla f\left(\theta_t\right)^\top v_i\right|} - \lambda_i\right) - 4L_t^i \cdot \left|\nabla f\left(\theta_t\right)^\top v_i\right|}{5\lambda_i \sqrt{\lambda_i^2 + 2L_t^i \cdot \left|\nabla f\left(\theta_t\right)^\top v_i\right|} - 5\lambda_i^2 - 8L_t^i \cdot \left|\nabla f\left(\theta_t\right)^\top v_i\right|} \cdot \Delta\Delta^i\theta'_t \\
&\left. + \frac{2\lambda_i \sqrt{\lambda_i^2 + 2L_t^i \cdot \left|\nabla f\left(\theta_t\right)^\top v_i\right|} - 2\lambda_i^2 - 2L_t^i \cdot \left|\nabla f\left(\theta_t\right)^\top v_i\right|}{5\lambda_i \sqrt{\lambda_i^2 + 2L_t^i \cdot \left|\nabla f\left(\theta_t\right)^\top v_i\right|} - 5\lambda_i^2 - 8L_t^i \cdot \left|\nabla f\left(\theta_t\right)^\top v_i\right|} \cdot \Delta\Delta^i\theta_t'^2 \right)
\end{aligned}
$$

Noting the common structure of each of the coefficients of $\Delta\Delta^i\theta_t'^1, \Delta\Delta^i\theta_t'^2, \Delta\Delta^i\theta_t'^3$, we prove the following to bound all three via appropriate settings of $a, b \in \{2, 4, 7, 12\}$:

If $\lambda_i > 0$:

$$
\begin{aligned}
&\lim_{\frac{L_t^i \cdot \left|\nabla f\left(\theta_t\right)^\top v_i\right|}{\lambda_i^2} \to \mathcal{L}} \frac{a\lambda_i \cdot \left(\sqrt{\lambda_i^2 + 2L_t^i \cdot \left|\nabla f\left(\theta_t\right)^\top v_i\right|} - \lambda_i\right) - bL_t^i \cdot \left|\nabla f\left(\theta_t\right)^\top v_i\right|}{5\lambda_i \sqrt{\lambda_i^2 + 2L_t^i \cdot \left|\nabla f\left(\theta_t\right)^\top v_i\right|} - 5\lambda_i^2 - 8L_t^i \cdot \left|\nabla f\left(\theta_t\right)^\top v_i\right|} \\
&= \lim_{\frac{L_t^i \cdot \left|\nabla f\left(\theta_t\right)^\top v_i\right|}{\lambda_i^2} \to \mathcal{L}} \frac{a\frac{2}{\sqrt{1+2\frac{L_t^i \cdot \left|\nabla f\left(\theta_t\right)^\top v_i\right|}{\lambda_i^2}}+1} - b}{5\frac{2}{\sqrt{1+2\frac{L_t^i \cdot \left|\nabla f\left(\theta_t\right)^\top v_i\right|}{\lambda_i^2}}+1} - 8} \\
&= \begin{cases} \frac{b-a}{3} & \mathcal{L} = 0^+ \\ \frac{b}{8} & \mathcal{L} = \infty \end{cases}
\end{aligned}
$$

If $\lambda_i \leq 0$:

$$
\begin{aligned}
&\lim_{\frac{L_t^i \cdot \left|\nabla f\left(\theta_t\right)^\top v_i\right|}{\lambda_i^2} \to \mathcal{L}} \frac{a\left|\lambda_i\right| \cdot \left(\sqrt{\left|\lambda_i\right|^2 + 2L_t^i \cdot \left|\nabla f\left(\theta_t\right)^\top v_i\right|} + \left|\lambda_i\right|\right) + bL_t^i \cdot \left|\nabla f\left(\theta_t\right)^\top v_i\right|}{5\left|\lambda_i\right| \left(\sqrt{\left|\lambda_i\right|^2 + 2L_t^i \cdot \left|\nabla f\left(\theta_t\right)^\top v_i\right|} + \left|\lambda_i\right|\right) + 8L_t^i \cdot \left|\nabla f\left(\theta_t\right)^\top v_i\right|} \\
&= \lim_{\frac{L_t^i \cdot \left|\nabla f\left(\theta_t\right)^\top v_i\right|}{\lambda_i^2} \to \mathcal{L}} \frac{a\left(\sqrt{1 + 2\frac{L_t^i \cdot \left|\nabla f\left(\theta_t\right)^\top v_i\right|}{\left|\lambda_i\right|^2}} + 1\right) + b\frac{L_t^i \cdot \left|\nabla f\left(\theta_t\right)^\top v_i\right|}{\left|\lambda_i\right|^2}}{5\left(\sqrt{1 + 2\frac{L_t^i \cdot \left|\nabla f\left(\theta_t\right)^\top v_i\right|}{\left|\lambda_i\right|^2}} + 1\right) + 8\frac{L_t^i \cdot \left|\nabla f\left(\theta_t\right)^\top v_i\right|}{\left|\lambda_i\right|^2}} \\
&= \begin{cases} \frac{a}{5} & \mathcal{L} = 0^+ \\ \frac{b}{8} & \mathcal{L} = \infty \end{cases}
\end{aligned}
$$

Analogously to the first case, and due to the monotonic natures (for all $a, b \in \mathbb{R}$) of

$$
\psi_3 : \mathbb{R}^+ \to \mathbb{R}, \psi_3\left(x\right) = \frac{a\frac{2}{\sqrt{1+2x}+1} - b}{5\frac{2}{\sqrt{1+2x}+1} - 8}
$$

and

$$
\psi_4 : \mathbb{R}^+ \to \mathbb{R}, \psi_4\left(x\right) = \frac{a\left(\sqrt{1+2x}+1\right) + bx}{5\left(\sqrt{1+2x}+1\right) + 8x}
$$

the term in the parentheses is bounded, thus we may conclude our proof of the lemma. □

Remark. *Note that when* $\lambda_i > 0$, $\frac{L_t^i \cdot \left|\nabla f(\theta_t)^\top v_i\right|}{\lambda_i^2} \to 0^+$, *the coefficients of* $\Delta\Delta^i{\theta'_t}^3, \Delta\Delta^i{\theta'_t}^1$ *shrink to 0 (since* $a = b$ *for those cases), so that* $\left|\frac{m_t^i\left(\Delta\theta_t^\top v_i\right) - m_t^i\left(\Delta\theta_t^{*\top} v_i\right)}{m_t^i\left(\Delta\theta_t^{*\top} v_i\right)}\right| = \Theta\left(\Delta\Delta^i{\theta'_t}^2\right)$

We are now ready to prove theorem 3.3.

Theorem. *Worst-case descent rate for arbitrary optimizers*

Let $f : \mathbb{R}^n \to \mathbb{R}$ *a twice-differentiable function satisfying assumptions 1 and 2, and let* $\Delta\theta_t$ *satisfy* $M_t^i\left(\Delta\theta_t^\top v_i\right) \leq 0$. *Then*

- $$\left|\frac{M_t^i\left(\Delta\theta_t^\top v_i\right)}{M_t^i\left(\Delta\theta_t^{*\top} v_i\right)}\right| = \Theta\left(1 + \left|\Delta\Delta^i{\theta'_t}\right|^2\right)$$

- $$\left|\frac{m_t^i\left(\Delta\theta_t^\top v_i\right)}{m_t^i\left(\Delta\theta_t^{*\top} v_i\right)}\right| = \Theta\left(1 + \left|\Delta\Delta^i{\theta'_t}\right|^p\right) \tag{20}$$

  with $p = \begin{cases} 2 & \lambda_i > 0 \wedge \frac{\left|\nabla f(\theta_t)^\top v_i\right|}{\lambda_i^2} = 0 \\ 1 & else \end{cases}$.

Proof. Proof is immediate from lemma M.5, because we have

$$\frac{M_t^i\left(\Delta\theta_t^\top v_i\right)}{M_t^i\left(\Delta\theta_t^{*\top} v_i\right)} = 1 + \frac{M_t^i\left(\Delta\theta_t^\top v_i\right) - M_t^i\left(\Delta\theta_t^{*\top} v_i\right)}{M_t^i\left(\Delta\theta_t^{*\top} v_i\right)}$$

and similarly for $m_t^i\left(\Delta\theta_t^\top v_i\right)$. □

N LIMITATIONS AND FUTURE WORK

One interesting direction for future research is in putting the estimated Lipschitz parameters to work throughout the optimization process to increase the descent rate in hopes of matching and even surpassing ARC's strong performance (Xu et al., 2017), i.e. applying algorithm ELMO in practice. We provide some basic methods for Lipschitz estimation in this paper, but future work may propose more accurate/low-overhead estimators. In this paper we focused primarily on the optimizer selection challenge, thus no experiments in this direction were attempted.

A second direction for future research is a bias correction for our simple Lipschitz parameter estimation in AMOS, much like Kingma & Ba (2014) did for Duchi et al. (2011a) and Tieleman & Hinton (2012). We also recall that the AMOS experiments in this work were performed on a per-tensor basis, but other partitions (e.g. constant chunk-size irrespective of tensor borders) may work better - no experiments were attempted in this direction.

One limitation of our Newton's method performance predictor is the additional computational burden of computing the Lipschitz parameters. While some algorithms (e.g. Sophia) explicitly compute all the Hessian eigenvalues, others do not, which poses challenges in computing Lipschitz parameters with minimal overhead. However since the Hessian is usually only estimated at large intervals, the additional cost of Lipschitz estimation may be amortized across these iterations.

A second limitation is the need to store a copy of the model parameters at the position at which the previous Hessian was estimated; this adds pressure to the memory, which may pose a bottleneck in settings with large models or activations. Many modern optimizers already hold several buffers the same size as the model, however (e.g. Adam, which stores the first- and second gradient moments), such that this copy does not affect the order of magnitude of storage required. Furthermore, certain training models already store previous copies of the model parameters (e.g. Allen-Zhu (2016)), such that this may not add any additional overhead.

A third limitation of our work is its inability to provide any indication of the number of iterations left to achieve convergence (unlike previous works which bound the gradient norm as a function of the number of iterations, which is a measure of convergence). We see this as an acceptable limitation however, since in practice a model is only required to achieve a certain level of performance on the data decided ahead of time, without regard to how much further it could be optimized. As noted in the introduction, performance is measured by the loss function, so our descent rate bound satisfies this practical requirement.

A final limitation of our bound is its reliance on $\Delta\Delta^i\theta_t$ as a measure of algorithm optimality which is a function of $\Delta\theta_t^{*\top} v_i$, despite the fact that most optimizers do not compute that during training. This bound is therefore primarily of theoretical interest, as illustrated by its motivation of the very practical metric discussed in section 4.